

Annual Review of Earth and Planetary Sciences

Fiber-Optic Seismology

Nathaniel J. Lindsey^{1,2} and Eileen R. Martin³

¹Department of Geophysics, Stanford University, Stanford, California 94305-2215, USA

²Current affiliation: FiberSense, Oakland, California 94619, USA;
email: nate.lindsey@fiber-sense.com

³Department of Mathematics, Virginia Polytechnic Institute and State University, Blacksburg, Virginia 24060, USA

Annu. Rev. Earth Planet. Sci. 2021. 49:309–36

First published as a Review in Advance on
January 5, 2021

The *Annual Review of Earth and Planetary Sciences* is
online at earth.annualreviews.org

<https://doi.org/10.1146/10.1146/annurev-earth-072420-065213>

Copyright © 2021 by Annual Reviews.
All rights reserved

Keywords

distributed acoustic sensing, seismology, fiber optics

Abstract

Distributed acoustic sensing (DAS) is an emerging technology that repurposes a fiber-optic cable as a dense array of strain sensors. This technology repeatedly pings a fiber with laser pulses, measuring optical phase changes in Rayleigh backscattered light. DAS is beneficial for studies of fine-scale processes over multi-kilometer distances, long-term time-lapse monitoring, and deployment in logistically challenging areas (e.g., high temperatures, power limitations, land access barriers). These benefits have motivated a decade of applications in subsurface imaging and microseismicity monitoring for energy production and carbon sequestration. DAS arrays have recorded microearthquakes, regional earthquakes, teleseisms, and infrastructure signals. Analysis of these wavefields is enabling earthquake seismology where traditional sensors were sparse, as well as structural and near-surface seismology. These studies improved understanding of DAS instrument response through comparison with traditional seismometers. More recently, DAS has been used to study cryosphere systems, marine geophysics, geodesy, and volcanology. Further advancement of geoscience using DAS requires several community efforts related to instrument access, training, outreach, and cyberinfrastructure.

- DAS is a seismic acquisition technology repurposing fiber optics as arrays of dynamic strain sensors at 1- to 10-m spacing over kilometers.
- Easy DAS installations have availed time-lapse geophysical sensing in formerly inaccessible sites: urban, icy, and offshore areas.
- High-frequency wavefields recorded by DAS are analyzed with array-based methods to characterize seismic sources and image the subsurface.

ANNUAL
REVIEWS **CONNECT**

www.annualreviews.org

- Download figures
- Navigate cited references
- Keyword search
- Explore related articles
- Share via email or social media

- DAS has shown low-frequency sensitivity in the laboratory and field, for slow hydrodynamic and geodynamic processes.

1. INTRODUCTION

Distributed acoustic sensing (DAS) is an emerging geophysical method that uses an optoelectronic instrument connected to an optical fiber to measure strain along the fiber, effectively repurposing it as a seismic array. The optoelectronic instrument, called an interrogator unit (IU), sends laser pulses into the optical fiber and measures subtle phase shifts in Rayleigh scattered light at each point along the fiber, as measured in the time or frequency domain. In this way, the strain field acting on a fiber coupled to Earth can be sampled at meter-scale spatial resolution over tens of linear fiber kilometers. In this review, we focus on fiber-optic DAS technology that yields an array of dynamic strain sensors, as opposed to other fiber-optic sensing technologies for geophysical monitoring such as in reviews by Marra et al. (2018) or Zhang et al. (2018).

DAS enables scientists to test hypotheses using high-density and large aperture experiments. Deploying traditional sensing systems (nodal arrays, geophones, seismometers) is not always logistically feasible due to space constraints, land access issues, extreme temperatures, or power limitations. By contrast, DAS is used to study a variety of geoscientific processes and locations (urban areas, offshore, glaciers, wells, volcanoes). A few installations are pictured in **Figure 1**. These experiments are being conducted by a growing number of institutions, primarily in North America and Europe, with some in Asia and Oceania.

For the past decade, DAS has been increasingly utilized in exploration geophysics related to the oil and gas industry, geothermal energy, and CO₂ sequestration. Much of this effort has focused on vertical seismic profile (VSP) imaging, time-lapse imaging, and continuous microseismicity monitoring, as well as some on geomechanical strain monitoring. Over the past 5 years applications have grown in near-surface geophysics for engineering, infrastructure, and environmental studies, particularly those requiring long-term monitoring. More recently, the use of DAS has grown into offshore marine seismology, glaciology, and geomechanics. The progression from DAS primarily being used for short-duration active source experiments to a mix of continuous monitoring and other applications can be seen in the time line of a sampling of DAS experiments in **Figure 2**. Note that researchers are increasingly collecting relatively high sample rate data for long durations, leading to data volumes per experiment that are much larger than traditional seismic experiments. For example, a sample of just nine experiments (a mix of lower-rate and higher-rate experiments) accumulated roughly 800 TB of data for applications ranging from near-surface geotechnical engineering to hydrology, geothermal monitoring, urban geophysics, and permafrost monitoring.

As DAS arrays have been used to acquire data in a wider variety of applications, a deeper understanding of DAS instrument response and the effect of optical fiber installation conditions has become important. Accordingly, methods for detecting signals, locating sources, and imaging the subsurface with both body and surface waves have required modifications to existing algorithms in order to accurately account for differences in recording data with a dynamic linear strain array. As DAS arrays have increased sensor density by 10 to 1,000 times and enabled acquisitions in many new environments with a wide variety of seismic sources, efficient computational methods have become increasingly important to the analysis.

Before DAS may be more widely utilized by geoscientists, a variety of community-scale challenges and needs must be addressed by the Earth science community. In particular, we review

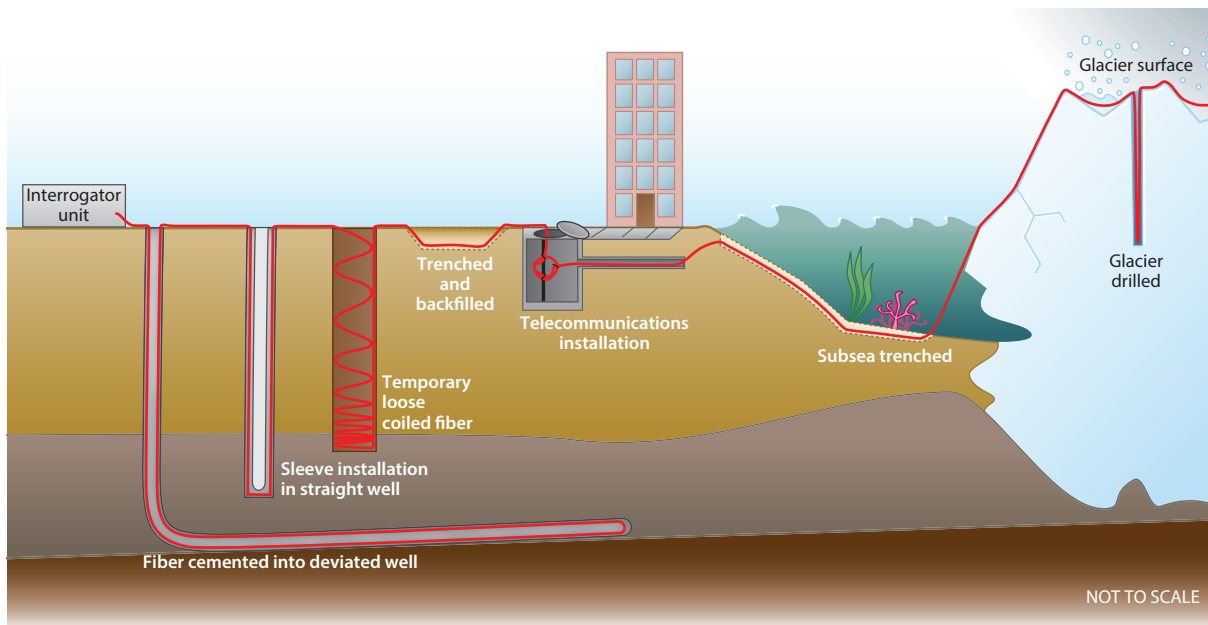


Figure 1

The same interrogator unit can be connected to fiber optics installed in a variety of ways on land, offshore, and even over ice. Some installation scenarios are pictured (from *left to right*): fiber cemented into a deviated well, an installation in a vertical well using a sleeve to push fiber against the sides, a temporary installment of coiled fiber, fiber laid in a shallow backfilled trench, fiber in underground telecommunications infrastructure, ocean bottom offshore fiber, fiber stretched across a glacier, and fiber installed in an ice borehole drilled with hot water. The figure is not to scale, as the maximum fiber distances probed with a single interrogator have been in the tens of kilometers.

challenges in instrument availability and access, reproducibility of results, data standards, large-scale data analysis, archival, and management.

2. DISTRIBUTED ACOUSTIC SENSING MEASUREMENTS

Direct strain measurements have been made for nearly 100 years (Benioff 1935), but distributed optical fiber strain sensing has developed over just the past few decades. Optical fibers were exploited for acoustic point-strain sensing beginning in the 1970s (Bucaro et al. 1977, Cole et al. 1977). Long-baseline optical interferometry with evacuated tubes was incorporated into geodesy around the same time (Berger & Lovberg 1970). Using an optical fiber light path for measurements of long-baseline strain greatly simplified interferometer construction (Zumberge et al. 1988). Today, field-based point-strain fiber-optic interferometry achieves nanostrain sensitivity and can detect tidal strain, tremor, and slow slip (Blum et al. 2008, DeWolf et al. 2015, Zumberge et al. 2018). DAS applies many of the same materials and methods as traditional optical strain sensing but generates an array of dynamic strain measurements.

2.1. Distributed Acoustic Sensing Measurement Principle

DAS refers to any method in which optical interferometry is applied to laser light traveling inside of an optical fiber to measure strain or strain rate at many positions along the fiber. DAS

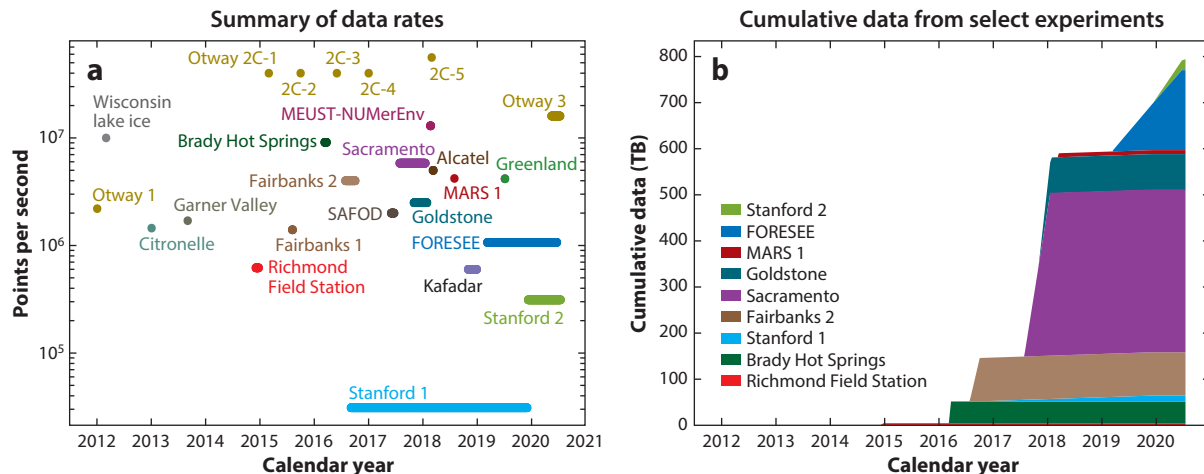


Figure 2

(a) A selection of experiments conducted by US national labs and universities shows that long-term monitoring experiments are becoming more common. Short-term experiments typically collect hundreds of thousands to millions of data points per second, while long-term experiments trade off this high sample rate for duration. (b) A sample of nine experiments from a mix of application areas accumulated roughly 800 TB of data. Abbreviations: FORESEE, Fiber-Optic for R Environment SEnsEing; MARS, Monterey Accelerated Research System; MUEST-NUMerEnv, Mediterranean Eurocentre for Underwater Sciences and Technologies–Neutrino Mer Environment; SAFOD, San Andreas Fault Observatory at Depth. Data from Daley et al. (2013); Lancelle (2016); Ajo-Franklin et al. (2017, 2019); Castongia et al. (2017); Dou et al. (2017); Martin (2018); Wang et al. (2018); Correa et al. (2019); Lellouch et al. (2019); Lindsey (2019); Williams et al. (2019); Yu et al. (2019); Booth et al. (2020); Lindsey et al. (2020); Luo et al. (2020); and Zhu et al. (2020).

is also referred to as distributed vibration sensing, coherent optical time-domain reflectometry (OTDR), coherent optical frequency-domain reflectometry (OFDR), or phase-sensitive OTDR. The DAS instrument is referred to as an optoelectronic IU and has a field form factor that fits on a workbench. All IUs generate, send, and receive laser pulses to and from an attached fiber sensor. Laser light commonly falls in the near-infrared wavelength range ($\sim 1,550$ nm) and is pulsed, but some DAS instruments use continuous and swept-frequency light sources. Refractive index heterogeneities in the fiber's silica glass core cause Rayleigh scattering as pictured in **Figure 3**. Rayleigh scattering is well characterized by the telecommunications industry because of its transmission impact, which can cause a drop in signal strength of 0.15–0.20 dB/km for near-infrared

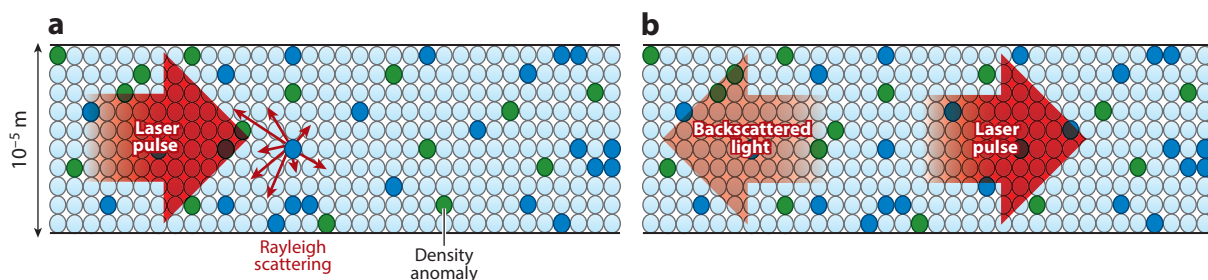


Figure 3

Diagram depicting (a) Rayleigh scattering event at sites of index of refraction change (blue/green) inside the core of a single-mode optical fiber laser. (b) Most light continues to propagate down the fiber, but distributed acoustic sensing utilizes the backscattered energy. Figure adapted from Lindsey et al. (2020).

wavelengths such as those commonly used for DAS. Only a small amount of the scattered light returns to the IU.

There are many ways to implement DAS. A common technique uses an IU to repeatedly inject laser pulses into an optical fiber and analyze the phase of the Rayleigh backscattered signal with OTDR. OTDR assumes the mean fiber path follows a simple out-and-back trajectory between the IU and Rayleigh scattering point. A known two-way travel time of light in the fiber provides the necessary information to map each subset of the backscattered profile in time to a subset of linear fiber distance. OTDR multiplexes the time-continuous backscattering into an array of independent signals returning from consecutive fiber segments, called gauges. The gauge length is the corresponding spatial increment of fiber sampled by each signal, typically about 1 to 40 m long (Dean et al. 2017). The spatial axis of a DAS data set is reported in channels at 0.5 m or less, often subset from the gauge length; however, spatial resolution is fixed by the gauge length.

Backscattering phases, as opposed to amplitudes, are proportional to the change in path length over the gauge length. DAS recordings capture dynamic strains at acoustic frequencies ($f > 1,000$ Hz) and broadband seismic frequencies ($f = 0.001 - 1,000$ Hz), and they have also shown promise for studies at ultra-low frequencies that would classically be called static strain or geodesy (periods of hours to weeks) but that relax away over long enough timescales (Becker et al. 2017, Becker & Coleman 2019).

2.2. Optoelectronic Interrogator

Inside the IU, optical interferometry is applied to the backscattered signal to measure phase or phase rate. The exact units depend on the particular DAS approach. Dakin (1990) described the first distributed optical strain sensing instrument. According to this approach, a pair of laser pulses separated in frequency (f_1 and f_2) are launched one after the other and the backscattered signal is measured at the beat frequency ($\Delta f = |f_1 - f_2|$). The temporal separation of the pulses results in a backscattered signal that combines light from location x_1 (first pulse) with location x_2 (second pulse) separated by the gauge length (Masoudi & Newson 2016). The backscattered signal phase $\Delta\Phi$ is linearly related to the gauge strain ϵ_{xx} , following

$$\epsilon_{xx}(t, \mathbf{x}) = \frac{\lambda}{4\pi n_c x_g \psi} \Delta\Phi, \quad 1.$$

where t and \mathbf{x} locate the axial strain measurement along the fiber axis ($+\mathbf{x}$ direction), λ is the frequency used for measurement (beat frequency here), n_c and ψ are the refractive index and Pockels coefficient of the single mode fiber glass ($\psi = 0.79$), and x_g is the gauge length (Hartog 2017). This assumes $\Delta\Phi$ is related only to the fiber's dynamic mechanical strain. Optical dispersion effects are easily considered for multifrequency setups or ignored for single-frequency ones. Thermo-optical effects and thermal strain are ignored because the deformation measurement timescale in seismology is much less than the thermal variation timescales; however, these must be accounted for in low-frequency DAS strain measurements or faster thermal cycles.

Posey et al. (2000) described an alternative approach that injects one pulse and analyzes the backscattering with a Mach–Zehnder interferometer and 3×3 coupler and measures the change in optical phase over time (optical phase rate). Here, gauge length is controlled by gating the backscattered signal, ultimately limited by pulse width (Farhadiroushan et al. 2009, Masoudi et al. 2013, Parker et al. 2014). A third approach, in the vein of Kishida et al. (2014) and Kreger et al. (2015), expands on the original ideas of OFDR proposed by Eickhoff & Ulrich (1981). The OFDR method is a single continuous swept-frequency method. When the backscattered signal is recombined with the light source, it generates a range of beat signals whose frequency is linearly related to fiber position. Cross-correlating OFDR traces is used to measure phase changes through time.

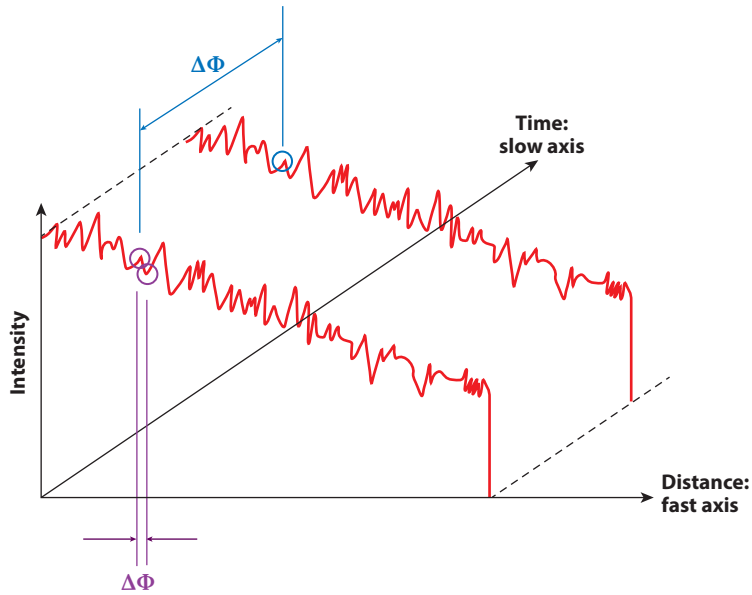


Figure 4

Intensity versus time and distance of two pulses demonstrates how the optical phase information for a gauge length can be computed as the phase change across a gauge measured using a single pulse along the fast axis or as the rate of phase change across a gauge between repeat pulses along the slow axis. Figure adapted from Masoudi & Newson (2016).

To summarize, DAS IUs measure the optical phase between consecutive gauges at a single time (one pulse)—that is, along the fast axis in **Figure 4**—or by mixing signals returning from the same gauge over two repeated laser pulses, termed the slow axis (Masoudi & Newson 2016). Along the fast axis the measurand is optical phase (strain). Along the slow axis the measurand is the change in phase per pulse separation time (strain rate).

2.3. Fiber-Optic Sensing Element

In the lab the DAS sensing element is simply the optical fiber through which the laser travels, but in the field the sensor response depends on how the fiber (core and buffer materials) is coupled to the surrounding Earth. Exploration of DAS strain transfer issues first appeared in VSP experiments where data quality was found to systematically improve with the degree of rigid coupling between free-hanging, clamped, and grouted fibers (Mestayer et al. 2011, Hartog et al. 2014, Kuvshinov 2016, Munn et al. 2017). Horizontally trenched direct-burial and telecommunications fiber installations face at least as many complications as vertical fiber installations. Added complications may include fiber cladding and jacket materials, gel lubricants and strength members (e.g., aramid yarn, steel-armor) embedded for strain support, exterior cable packaging, the exterior cable texture, soil cohesion, and the use of any conduit or borehole materials. At present, these complications are not fully understood and are a topic of active research.

2.4. Distributed Acoustic Sensing Instrument Response

As DAS technology improved to enable geophone-level data quality for applied geophysics from roughly 2010 to 2014 (Mestayer et al. 2011, Daley et al. 2013, Frignet et al. 2014, Mateeva et al.

2014, Bakku 2015), the physical meaning of DAS measurements received increased attention. One simple model of DAS strain rate measurements is equivalent to the difference of two inertial velocity sensors separated by the gauge length (Daley et al. 2016). Wang et al. (2018) proved this in the field by comparing earthquake records from geophones differenced across a short fiber span. DAS amplitude response functions include notches associated with seismic wavelengths that apply zero strain at integer multiples of the gauge length, so the gauge length must be selected appropriately for the application (Bona et al. 2017, Dean et al. 2017, Jousset et al. 2018, Martin et al. 2018b). Lindsey et al. (2020) provided an alternative description in terms of optical interferometry, wherein the measured optical phase is directly related to the longitudinal fiber strain. Aside from the notch effect at short periods, DAS with a straight cable provides a response that is theoretically flat in phase and amplitude.

Field experiments have verified the exceptional broadband frequency response of DAS. High sampling rates and stable lasers improved capabilities to record microearthquake signals above 300 Hz (Baird et al. 2020, Lellouch et al. 2020a), urban noise from vehicles around 8–30 Hz (Dou et al. 2017), microseism energy from ocean–solid Earth interactions (Lindsey et al. 2019, Sladen et al. 2019, Williams et al. 2019), 20- to 300-s period teleseismic recordings (Lindsey et al. 2017, 2019; Ajo-Franklin et al. 2019; Yu et al. 2019), and tidal periods (12 h) produced in the laboratory (Becker & Coleman 2019).

DAS self-noise is commonly described as being roughly $10^{-11} - 10^{-8} \epsilon/\sqrt{\text{Hz}}$ (10 piconstrain – 10 nanostrain) depending on optical setup, gauge length, range, frequency, and laser noise. Spurious optical noise has not been rigorously evaluated by the geophysics community, but observations have been noted, including common-mode noise related to mechanical vibration of the IU (Hartog 2017), random impulse noise attributed to the laser (Zhirnov et al. 2016), optical fading or reduced amplitudes at quasi-random locations resulting from destructive optical interferometry (Zhou et al. 2013, Gabai & Eyal 2016), and drift (Becker & Coleman 2019). Optical fading and poor coupling of a channel are indistinguishable except at the scale of the array, where coupling issues are often identifiable by systematic patterns or field installation information.

Straight fibers have strong azimuthal sensitivity similar to linear strainmeters, falling off like $\cos^2(\theta)$ rather than $\cos(\theta)$ in response to longitudinal waves, where θ is the angle formed between the wave vector and the fiber's axis (Benioff 1935). Also like the strainmeter, sensor polarity is more complicated than standard geophones (Lindsey et al. 2017). Alternatively, cables can be designed with helically wound fibers around a central mandrel to provide sensitivity to longitudinal waves from a wider range of angles (Kuvshinov 2016, Lim Chen Ning & Sava 2018).

Sensor coupling is critical for any seismic instrument. Laboratory tests show significantly weaker responses for loosely bonded and gel-filled fiber in metal tube sensors relative to cemented bare fiber (Papp et al. 2017, Becker et al. 2018), yet surface waves are routinely observed with fiber packages deployed in shallow trenches in urban areas (Dou et al. 2017, Martin et al. 2017a), or even in deployments on the surface simply weighed down temporarily (Spikes et al. 2019). Careful DAS amplitude response calibration using colocated reference has found a 5- to 10-dB elevated amplitude response at frequencies above 0.1 Hz for many teleseismic earthquakes and nighttime microseism recording (Lindsey et al. 2020), suggesting coupling must be considered for full-waveform and amplitude-based DAS studies.

2.5. Field Practice

As outlined in **Figure 1**, there are a wide variety of installation techniques that are often specific to the environment being studied, and best practices are still an area of active research. Once fiber is installed, locating DAS fiber channels in real coordinate space requires tap-testing with a

hammer at known global positioning system points during recording. Depth information is known either from directly burying the cable or from the cable operator/owner. End points and midpoints of a direct-burial experiment are enough to register to within a precision of plus or minus half the gauge length. In dark fiber experiments, less information is available. Cable excess may be dispatched in utility holes, and splices may be undocumented (Martin 2018, Zhu & Stensrud 2019).

Most IUs require experimentalists to choose a laser pulse firing rate, and this rate is limited by ensuring that the light from one measurement has reached the end of the fiber and returned to the IU before the next measurement begins. The maximum pulse repetition rate f_R can be calculated from the refractive index n , and a known fiber length L , as

$$f_R = \frac{1}{L} \frac{c}{2 \cdot n}.$$

For example, in 1-km well-based DAS experiments, f_R could be set in the tens or hundreds of kilohertz. However, at 100 kHz the Nyquist frequency (50 kHz) exceeds the probable active source seismic frequency range (5–5,000 Hz depending on the experiment). For a 5-km fiber typical of direct-burial installations, $f_R \sim 35$ –50 kHz, which is still high compared to ambient, earthquake, and environmental seismic frequency ranges (0.002–200 Hz). In both of these experimental types, there is still photonic energy at the far end of the fiber, and thus fibers must be properly terminated to reduce backend reflection. For long-haul dark fiber telecommunication fiber, which can exceed 40 or 50 km, $f_R \sim 1$ –2 kHz so Nyquist is 500–1,000 Hz, which becomes potentially problematic for some applications (see **Figure 5**).

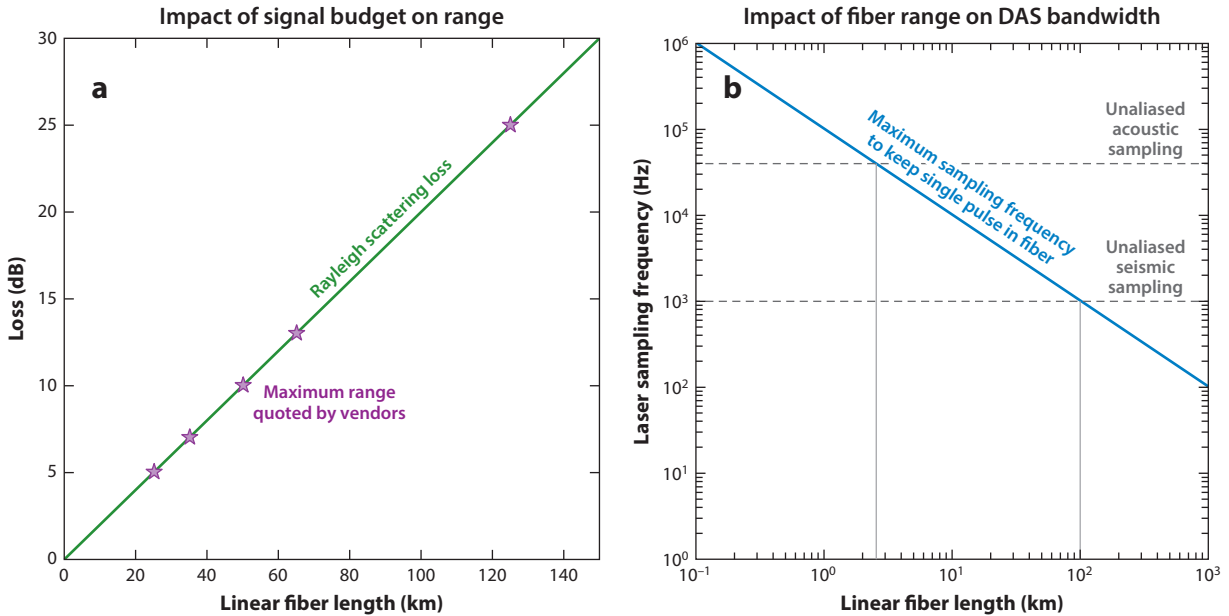


Figure 5

(a) The loss versus length relationship (green line) for standard telecommunications fiber (0.2 dB/km) is plotted with the maximum fiber lengths quoted by some DAS instrument vendors. (b) Optical interferometry requires clearing the first pulse before sending the second, creating a limitation in the pulse rate at which DAS can be used to sample the fiber that is based on the total fiber length. Abbreviation: DAS, distributed acoustic sensing.

3. ACTIVE AND PASSIVE CRUSTAL IMAGING

Whether the aim is mapping seismic velocity structure or reflectivity (velocity discontinuities), a common limiting factor in data acquisition for crustal-scale imaging is aperture (total size across the array and spacing between sensors). Exploration-scale imaging requires unaliased seismic waves in the 5–100 Hz range. Near-surface imaging for geotechnical engineering, earthquake hazards, or hydrological targets often demands lateral resolution of tens to hundreds of meters across cities or larger regions. At both scales, DAS has been a useful technique.

3.1. Exploration-Scale Imaging

VSP imaging uses an array of seismic sensors deployed in a well at 1–2 km depths, sometimes deeper. These sensors detect controlled sources at the surface (such as a walkaway VSP survey) or deployed in another well (a crosswell VSP survey). A primary limitation in traditional VSP studies has been the need to deploy wireline cables with a collection of geophones at specific levels. Crews set off a shot (controlled active seismic source), move the geophones' depth, and repeat the shot again several times to cover the full range of the target. Shot repeatability issues led to increased uncertainty in seismic data, so recording each shot along the whole length of a well instrumented with fiber is a major advantage. DAS allows scientists to use lower-amplitude sources or reduce acquisition time by using fewer repeated shots (Mateeva et al. 2017).

The majority of DAS recordings in the energy industry, at CO₂ sequestration sites and geothermal fields, have been performed in a downhole environment for VSP imaging (Mestayer et al. 2011; Mateeva et al. 2012, 2013a; Daley et al. 2013). Occasionally these systems are also used to monitor microseismicity or fluid flow through production (Webster et al. 2013, Bakku 2015, Karrenbach et al. 2017). Some examples of data and resulting images are shown in **Figure 6**. A series of studies compared noises and data quality expected for multiple installation techniques. Cables clamped to the side of a well performed better than loose straight cables. Cemented cables performed better than clamped cables (Mateeva et al. 2012). Cables with enough slack to touch the sides of a well may sometimes perform adequately (Constantinou et al. 2016). Data from fiber in tubing in fluid-filled boreholes show strong tube wave reverberations. Fiber deployed on casing with a mix of cemented and uncemented zones at the Ketzin, Germany, CO₂ site yielded poorer data quality in uncemented sections than in cemented sections (Daley et al. 2013, 2016; Egorov et al. 2017; Correa et al. 2019; Yavuz et al. 2019).

Obtaining a high-quality subsurface image once is a challenge, but a major driving factor in DAS technology development was the need to monitor time-lapse subsurface changes over years or decades. If geophysical methods can accurately detect subtle seismic velocity changes in thin layers (tens of meters) due to fluid displacement throughout production or isolate geomechanical changes due to production, engineers use these updated models to adjust production plans and reduce uncertainty in estimates. Repeatability errors in sensor locations and seismic sources often compounded to result in imaging uncertainties larger than the resolution and detection threshold required for the subtle, localized seismic velocity changes of interest (Mateeva et al. 2017). In addition to improving overall data quality, the use of DAS reduced the cost of every additional time-lapse survey, increasing the temporal resolution of monitoring to isolate changes due to specific production strategies (Mateeva et al. 2014, Harris et al. 2017, Kiyashchenko et al. 2020). At CO₂ sequestration sites, the cost constraints on monitoring for potential leakage from target zones require fully automated low-cost solutions, including DAS (Daley et al. 2007).

To extend array coverage, researchers can mix surface arrays with downhole arrays, as was done at the Ketzin CO₂ sequestration site (Daley et al. 2013). Later at the Otway site in Otway Basin, southern Australia, scientists acquired over 40 km of DAS surface and subsurface time-lapse data

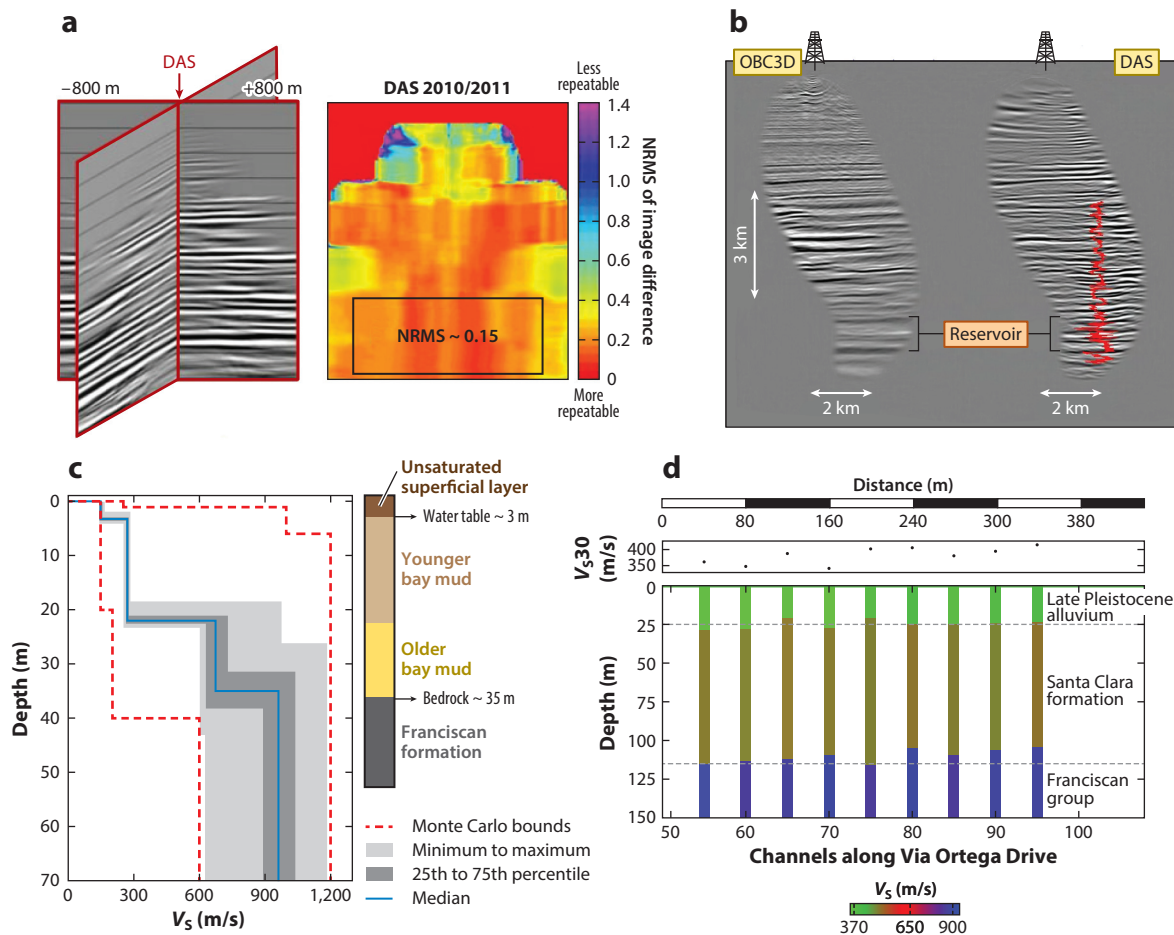


Figure 6

(a, left) Onshore VSP imaging with sources in an X-shaped configuration shows high resolution. (a, right) Time-lapse imaging maintained low RMS error in part due to sensor location repeatability. Panel a adapted from Mateeva et al. (2014). (b, left) Compared to ocean bottom cables, (right) three-dimensional DAS VSP at an offshore reservoir shows finer detail at the target and correlation to density logs. Panel b adapted from Shan et al. (2015). (c) Near-surface imaging using vibrations from a road recorded by a horizontal DAS array shows close correlation to directly measured geology. Panel c adapted from Dou et al. (2017). (d) Near-surface imaging with ambient noise recorded on a telecommunications array, and incorporating sparse seismometers, shows V_{S30} can vary significantly at the scale of tens of meters. Panel d adapted from Spica et al. (2020). Abbreviations: DAS, distributed acoustic sensing; NRMS, normalized root mean square; OBC3D, 3D Imaging with Ocean Bottom Cable instruments; RMS, root mean square; VSP, vertical seismic profile.

(Daley et al. 2013, Egorov et al. 2017, Correa et al. 2019, Yavuz et al. 2019). Also at the Otway site, researchers showed that time-lapse full-waveform inversion (FWI) imaging could be used to target a layer just 20 m thick where injection had the greatest effect (Egorov et al. 2017). While this study suggests that FWI can be applied to DAS VSP data, further application of FWI imaging to DAS data has been limited.

3.2. Near-Surface Ambient Noise Imaging

Ambient noise interferometry is a technique to use continuously recorded seismic wavefields from random sources to estimate signals mimicking active source seismic data. These signals between

sensor pairs are called noise correlation functions and (under ideal assumptions about the source distribution) estimate the wave equation's Green's functions. Typically, ambient noise analysis has been performed on signals below 1 Hz recorded by permanent arrays of sensors tens to hundreds of kilometers apart for regional-scale imaging (Shapiro & Campillo 2004). Several studies have applied this method to data acquired by dense, temporary, nodal arrays at frequencies approaching 2–3 Hz for near-surface imaging across kilometers (Schmandt & Clayton 2013). Higher frequencies and denser sensor spacing in DAS data could image properties in the top few tens of meters relevant to geotechnical engineering and earthquake hazard analysis for smaller buildings.

The sensitivity of ambient noise interferometry recorded by DAS arrays differs from traditional seismometers. For some sensor pairs, such as two collinear fiber channels, DAS is more robust to nonideal noise distributions than seismometer arrays. But for other geometries, such as two parallel channels, DAS interferometry can lead to false apparent velocity shifts. Simple models of common surface DAS array geometries show that one can select a subset of fiber channel pairs in the array, which yield accurate noise correlation functions (Martin et al. 2018b). Alternatively, estimating the seismic noise source distribution alongside modeling DAS sensor response can yield improved results throughout an array (Paitz et al. 2018).

In practice, passive seismic DAS data have been used successfully for near-surface imaging, often with vehicles as noise sources. A trenched and backfilled DAS array in Richmond, California, yielded stable Rayleigh wave signals within 8 h, and stochastic inversion with multichannel analysis of surface waves (MASW) yielded a subsurface model matching direct soil measurements (Dou et al. 2017). Surface waves from vehicles were similarly detected in agreement with nodes at a geothermal site in Garner Valley, California, and the results were used for tomographic imaging (Lancelle 2016; Zeng et al. 2016, 2017). Depending on geometry, clear dispersion images can be calculated from interferometry of relatively short recording periods (Martin et al. 2015) or limited car recordings (Yuan et al. 2020), but often clear surface wave signals can be extracted from ambient noise only after careful processing, such as to remove cars and normalize signals (Martin 2018, Martin et al. 2018a).

As done at the Stanford Phase 1 array, Rayleigh wave dispersion curves can be combined with vertical broadband seismometer data to find high-resolution estimates of horizontal to vertical spectral ratios, a quantity used to estimate site amplification of earthquake ground motions (Spica et al. 2020). Resulting V_{S30} (the S-wave velocity at 30 m depth) models showed variations at the scale of just a few tens of meters. Through ambient noise analysis with MASW imaging, geophysicists estimated V_{S30} on a dark fiber array stretching west from Sacramento, California. These one-dimensional (1D) profiles also showed that V_{S30} can vary significantly over distances less than 100 m (Ajo-Franklin et al. 2019, Rodríguez Tribaldos et al. 2020). These scales of variation are not currently captured by earthquake microzonation for building codes, so further research is required to understand how to incorporate fine-scale seismic velocity variations into larger-scale earthquake hazard maps.

Ambient noise seismology is increasingly being applied to hydrogeology. Monitoring watersheds with ambient noise has been carried out with sparse arrays of traditional seismometers (Clements & Denolle 2018), and a handful of attempts have been made to similarly utilize DAS. The Stanford Phase I array was used for near-surface imaging, and time-lapse ambient noise interferometry showed stronger amplitudes across longer distances, but this did not translate to velocity changes correlated to rainfall patterns, and nonideal anthropogenic noise was problematic (Martin 2018). There has been at least one success: Ambient noise data from a dark fiber array west of Sacramento were used to measure water table depth through S-wave velocity imaging. The resulting layered models agreed with ground truth measurements of soil type and water table depth. However, when testing time-lapse change detection, the submeter changes in water

table depth that were predicted based on rainfall were too small to resolve (Ajo-Franklin et al. 2019). More research is needed on spatial and temporal resolution of time-lapse ambient noise interferometry, especially above 1 Hz on DAS systems.

4. EARTHQUAKE SEISMOLOGY

Seismic arrays of 10–20 stations constructed to detect and beamform earthquake energy have been in operation for more than 50 years (Rost & Thomas 2002). Large-N seismic arrays composed of hundreds to thousands of seismic sensors have recently become widely used tools for earthquake seismologists (Lin et al. 2013, Schmandt & Clayton 2013). Large-N enabled studies of crustal structure, volcanoes, fault rupture of local and regional earthquakes, rivers, geysers, and urban seismology, but continuous performance is operationally prohibitive. Major challenges include power and storage demands, theft risk, labor, and operation and maintenance costs. Low-power sensors, low-cost sensors, and smartphone arrays may circumvent these issues (Kong et al. 2016) but currently span only short-period frequencies with high self-noise levels. Overcoming these challenges could extend, densify, and unlock new images of seismic wavefields such as on ice sheets and across spans of the seafloor, providing new opportunities to study the structure of the planet and understand the physics of earthquakes and seismic wave propagation.

Regularly spaced, dense DAS channels enable back projection and beamforming to extract stronger signals, as well as simple transformation between time-distance and frequency-wavenumber (f - k) domains. The array-nature of DAS recording enables improvements in template matching and machine learning algorithms over traditional seismic networks because unaliased wavenumber information reveals details of individual seismic phase refraction, reflection, and transmission. While the potential to deploy DAS on fiber networks for earthquake studies is high, this application faces two important challenges: single-component sensing and limited knowledge of instrument response.

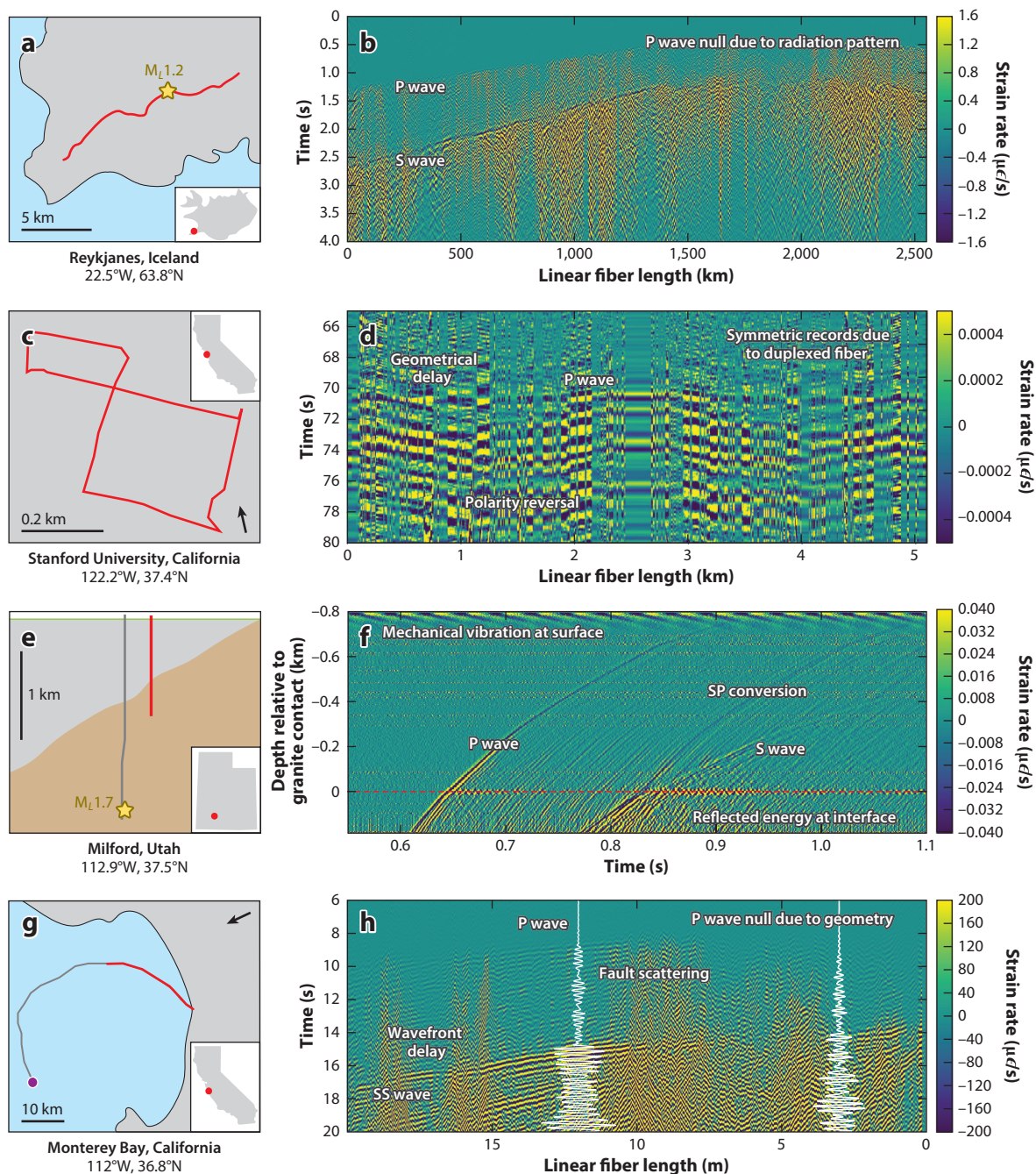
4.1. Event Detection

Numerous studies have used DAS to identify seismic events in applications ranging from down-hole microseismic monitoring to local, regional, and teleseismic recording. Some examples are shown in **Figure 7**. The need for seismic ground motion data across a breadth of applications demands instruments that detect particle velocities as small as $1\text{e-}9$ to $1\text{e-}6$ m/s, and stable recording of frequencies from millihertz to tens of kilohertz.

Local, regional, and teleseismic earthquake wavefields have been recorded using horizontal and vertical fiber-optic arrays deployed for DAS recording at many different sites following research by Lindsey et al. (2017), Martin et al. (2017b), Wang et al. (2018), Zhu & Stensrud (2019), Fang et al. (2020), Fernández-Ruiz et al. (2020), Luo et al. (2020), and Zhu et al. (2020). Common findings include accurate arrival time estimation of P and S waves, Love and Rayleigh wave group and phase velocity estimates, and consistent observations of coda envelopes. Combining information from many nearby DAS channels can improve detection by reducing local seismic noise. Template matching can also be used to extract additional events in order to better characterize the seismogenic process or delineate faults (Li & Zhan 2018). Observations of global earthquakes down to a 200-s period suggest that DAS can supplement existing sparse seismometer networks to study the planet's deep interior (Lindsey et al. 2017, Jousset et al. 2018, Ajo-Franklin et al. 2019, Yu et al. 2019). In one case, reflected PP wave energy was identified after weak P-wave arrival, likely due to the vertical-incidence broadside arrival over the horizontal optical fiber (Ajo-Franklin et al. 2019). DAS recordings of earthquakes with telecommunications

cables have been used in as many experiments to date as directly buried cables, although the specific differences in terms of instrument response are presently unknown.

In the oil and gas industry, small magnitude ($M < 2$) earthquakes are routinely recorded using DAS and used to monitor subsurface fluid injection and extraction activities (Webster et al. 2013,



(Caption appears on following page)

Figure 7 (Figure appears on preceding page)

(a,b) Fiber cable geometry (*red line*) and March 17, 2015, M_L 1.2 earthquake (*star* in panel a) from the Reykjanes Peninsula, Iceland. Panels a and b adapted from Jousset et al. (2018). (c,d) Stanford University campus fiber array used for DAS with the October 12, 2016, M_L 1.6 quarry blast wavefield record. Panels c and d adapted from Fang et al. (2020). (e,f) Cross section of FORGE monitoring Well 78-32 fiber (*red line*) and EGS stimulation well (*gray line*) and April 27, 2019, M_L 1.7 earthquake (*star* in panel e, *wavefield* in panel f). Panels e and f adapted from Lellouch et al. (2020a). (g,h) Monterey Accelerated Research System Cable in Monterey Bay, California (*red section* used for DAS), with March 10, 2017, M_w 3.4 Gilroy, California, earthquake recording. Arrows in panels c and g show two-dimensional epicenter-to-array vector. Panels g and h adapted from Lindsey et al. (2019). Abbreviations: DAS, distributed acoustic sensing; EGS, Enhanced Geothermal System; FORGE, Frontier Observatory for Research in Geothermal Energy.

Jin & Roy 2017, Karrenbach et al. 2018). The wavefield recordings from hydraulic fracturing operations provide additional information about the shale properties and state of stress in the local area (Cole et al. 2018, Baird et al. 2020, Lellouch et al. 2020b).

4.2. Wavefield Analysis

Recent DAS observations of atmosphere-ground coupling during storms, quarry blasts, and ice-quakes suggest that the utility of DAS touches many diverse fields of Earth science (Zhu & Stensrud 2019, Fang et al. 2020, Walter et al. 2020). DAS is unique in how it provides an efficient way to record wavefield information that can be analyzed with the tools of array processing to pick out complicated seismic conversions, infer source locations, and study local structure. Beamforming and back projection methods have been adapted to horizontal DAS data sets to assess the origin of seismic waves (Lindsey et al. 2017, Zhu & Stensrud 2019). Even in a vertical well, DAS earthquake recordings analyzed with a slant-stack algorithm provided some information on medium velocities and source directionality, such as velocity gradient measurements from up-going P- and S-wave analysis, as in **Figure 8** (Lellouch et al. 2019).

5. GEOPHYSICS FOR INFRASTRUCTURE AND URBAN AREAS

Fiber optics can be attached to or buried beside roads, railways, runways, and levees, making DAS a natural fit for sensing near-linear infrastructure across long distances. The ability to plug an IU into existing unused (so-called dark) telecommunications fiber has enabled easy access to urban locations where traditional seismic acquisition systems would be prohibitively difficult or costly to deploy. Seismic background noise in these areas varies significantly between sites, but DAS arrays' density enables targeted detection of local noise sources such as vehicles, footsteps, and trains.

5.1. Noise in Populated Areas

The anthropogenic seismic background has been studied using traditional sensors for decades, but DAS arrays have enabled us to capture the seismogenic processes taking place inside of urban areas in unprecedented detail for extended durations. Utilizing existing telecommunications infrastructure has enabled many more experiments throughout cities and college campuses. The signals at each are pictured in **Figure 9**. The first dark fiber experiment for seismology occurred in March 2015 in southwestern Iceland, and in some parts of the array, vehicle vibrations were much stronger than earthquake events (Jousset et al. 2018). In early 2016, scientists at Lawrence Berkeley National Laboratory carried out a trial dark fiber experiment by plugging a DAS interrogator into the Energy Sciences Network, or ESnet, fiber optics between Oakland and Berkeley, California (Ajo-Franklin et al. 2019). However, signals were dominated by nearby train movements and appeared to have little coupling to the subsurface. Fiber optics were installed in existing

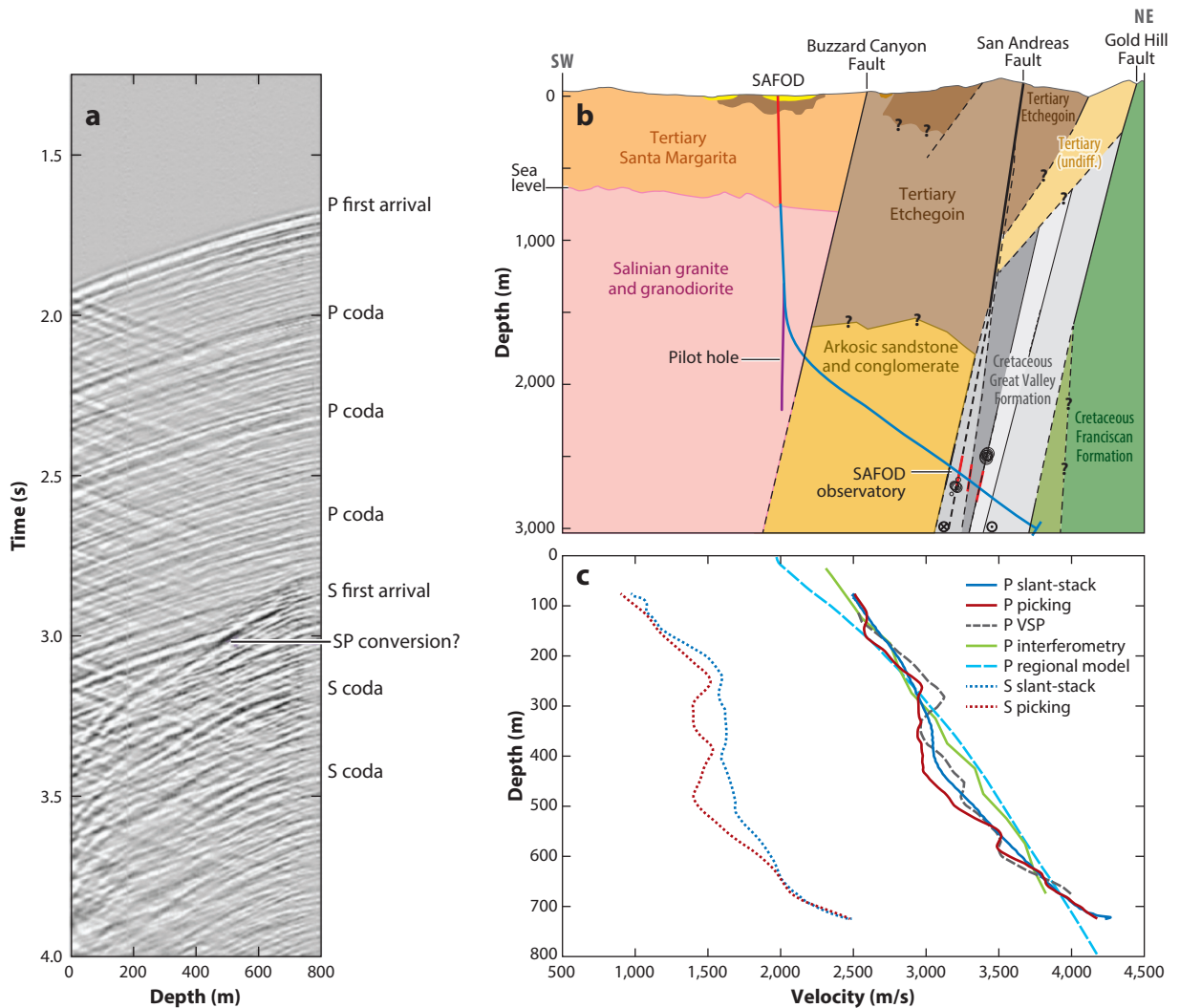


Figure 8

(a) DAS observation of an M_w 2.46 earthquake in the SAFOD borehole (BP = 0–120 Hz). The earthquake occurred at 11.16 km depth and 1.87 km away from the wellhead. (b) Geological cross section of the SAFOD borehole (red segment used for DAS). (c) Estimated P- and S-wave velocity models computed by DAS earthquake analysis (blue, slant-stack; red, travel-time picking; green, interferometry) plotted alongside P-wave VSP model (gray dashed line) and regional geologic model (cyan dashed line). Abbreviations: DAS, distributed acoustic sensing; SAFOD, San Andreas Fault Observatory at Depth; VSP, vertical seismic profile. Figure adapted from Lellouch et al. (2019).

telecommunications conduits under Stanford, California, and a wider variety of signals, some with daily and weekly trends, were observed from mid-2016 through mid-2019. These signals included vehicles, blasts from a nearby quarry (Biondi et al. 2017, Fang et al. 2020), construction site activities, and narrow-band signals from mechanical systems such as plumbing or HVAC systems (Martin 2018). A larger dark fiber array around Sacramento observed signals from vehicles and trains (Ajo-Franklin et al. 2019, Rodríguez Tribaldos et al. 2020). At a fit-for-purpose trenched array in Golden, Colorado, researchers observed strong high-frequency steam tunnel signals on

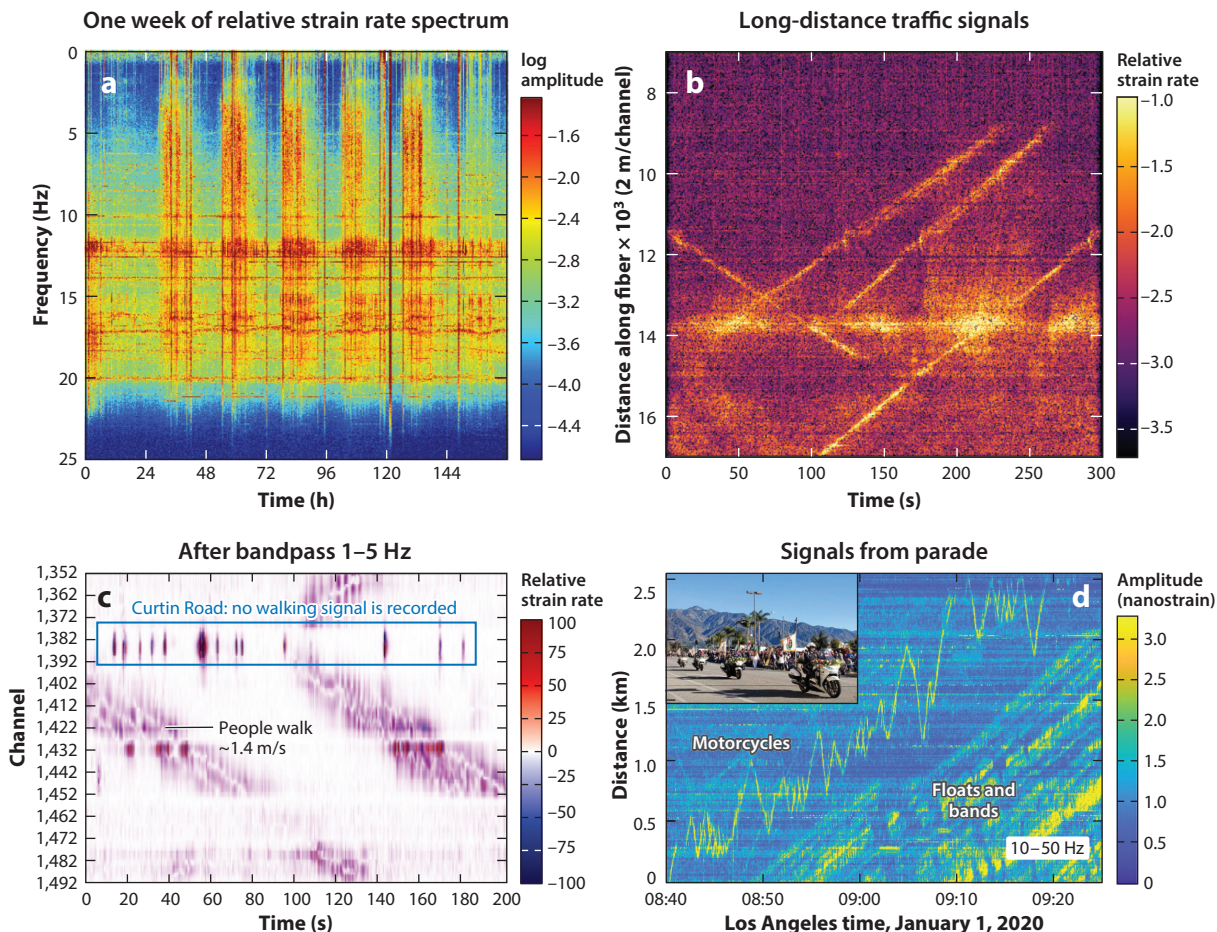


Figure 9

(a) One-week spectrum on a college campus shows diurnal, primarily weekday, anthropogenic signals and more constant narrow-band infrastructure signals. Panel *a* adapted from Martin (2018). (b) Vehicles on a road alongside an array are detected as 4 strong diagonal lines indicating speed. A pump system around 14 km along the fiber acts as a loud, stationary source. Signals are quiet at 7–9 km where the fiber and road are over 1 km apart. Data in panel *b* from Ajo-Franklin et al. (2019). (c) Individual footsteps have been detected in vehicle-free areas. Panel *c* adapted from Jakkampudi et al. (2020). (d) A variety of vehicles including motorcycles, floats, and bands were observed during a parade. Panel *d* adapted from Wang et al. (2020).

parts of the array (Luo et al. 2020). In another dark fiber array in State College, Pennsylvania, the familiar vehicle signals were detected, as well as musical vibrations from a concert and individual footsteps (Jakkampudi et al. 2020, Zhu et al. 2020). A parade passing over a dark fiber array in Pasadena, California, proved a rich source of noises including marching bands, floats on vehicles, and motorcycles (Wang et al. 2020). At each of these research sites, learning about the local seismic noise field has created a major bottleneck in exploring and preprocessing data, and these urban noise profiles may change over time as cities grow and change. Ultimately, widespread use of DAS systems for urban geophysics requires incorporation of automated tools to speed up data exploration, either through unsupervised learning (Martin et al. 2018a) or through models of well-characterized common noise sources as has been done for vehicles and footsteps along arrays (Huot et al. 2018a,b; Jakkampudi et al. 2020; Lindsey et al. 2020).

5.2. Urban Vehicle Tracking

Common sources of seismic waves in populated areas and around infrastructure are the vehicles driving along roads. On sparse seismometer arrays, signals are often thrown out if there is a local noise. In areas where vehicles hit bumps (either intentional road joints or cracks in the asphalt or pavement), additional surface waves are set off at approximately regularly timed intervals, which can wreak havoc on ambient noise interferometry (Martin et al. 2016). The high density of DAS allows us to distinguish between local signals and filter them. Simple unsupervised machine learning methods such as k -means clustering can reveal vehicle signals that are distinctive in the wavelet domain (and can thus be removed) (Martin et al. 2018a). Further accuracy improvements in automated vehicle detection were achieved through using convolutional neural networks, warm starting the optimization of network weights (i.e., transfer learning), and augmenting training data with synthetic vehicle signals (Huot et al. 2018a,b).

Vehicles are often treated as noise to be removed, but depending on array and road geometry, vehicles can sometimes be desirable sources of energy. In Richmond, California, noise correlation functions from a surface DAS array orthogonal to a road were calculated for time windows when vehicles were detected and used to produce a 1D image of the near surface that matched direct subsurface measurements (Dou et al. 2017). That analysis primarily used signals above 2 Hz, with surface waves emanating away from the road, but scientists have also gained valuable information from lower-frequency signals. These signals, noted by Huot et al. (2018a), were later modeled and explained by static strain as the roadbed deflection caused by the four wheels of a vehicle supporting the vehicle's mass (Jousset et al. 2018). Detecting car locations on a DAS array has also started being used to investigate spatially varying human movement patterns during pandemic lockdowns (Lindsey et al. 2020). The standard method to monitor traffic patterns is cell phone geolocation data, which risks the privacy of individuals, but DAS-based recording enables tracking public infrastructure use patterns without personally identifiable information.

5.3. Railbed Monitoring

Through use of fibers coupled to railbeds, 1- to 150-Hz DAS recordings have been used to monitor train position, speed, size, and railbed wear, defects, and deflection (Minardo et al. 2013, Peng et al. 2014, Timofeev 2015). Compared with conventional railbed point sensors and rail deflection monitoring tools, DAS enables continuous state-of-health information. For example, DAS has been used to create finely resolved profiles of moving train transient behavior by frequency domain analysis (Cedilnik et al. 2018). Recently, support vector machine and artificial neural network algorithms have demonstrated 10-fold speedups in this process and more robust handling of changing velocities (Kowarik et al. 2020, Wiesmeyr et al. 2020).

Short segments of DAS mounted on rails can measure in situ linear and nonlinear rail stiffness by recording dynamic shear forces due to loading from freight cars of known mass (Wheeler et al. 2019). While highly variable conditions of rail supports complicate this application, the multi-kilometer extent of DAS offers potential improvement in this technique's performance (Milne et al. 2020). Trains are a powerful source of anthropogenic seismic energy, with a peak signal around 2–5 Hz detected at distances over 50 km from railways (Inbal et al. 2018). DAS-based surface wave imaging studies can utilize these long-range train-induced coherent seismic waves to sample deeper structures than conventional vehicle-based surface wave analysis (Rodríguez Tribaldos et al. 2020).

5.4. Structural Health Monitoring

In addition to near-surface monitoring and understanding use patterns in urban areas, dense seismic arrays could enable better understanding of the movements and condition of bridges,

buildings, and other structures. After the establishment of baseline vibration behaviors, repeat studies after earthquakes or floods or during permafrost thaw could inform decisions about structural safety and reinforcement (Wagner et al. 2018, Lindsey 2019). Instrumentation of a university building with 200 point accelerometers allowed researchers to measure interface-wave dispersion and more accurately localize vibration events (Woolard & Tarazaga 2018). The DAS array in Pasadena presents unique opportunities to combine data simultaneously acquired by highly instrumented multistory structures with dense subsurface wavefield data (Martins et al. 2019, Wang et al. 2020).

Thus far in structural health monitoring, fiber-optic sensing has primarily been used to measure static strain and temperatures using Brillouin- and Raman-based techniques. In particular, embedded fiber optics have been used to monitor stresses in concrete pilings (Pelecanos et al. 2018), detecting when dams are being displaced, locating corrosion and leaks in pipelines, localizing cracks, guiding maintenance of historical buildings (Soga & Luo 2018), and detecting delamination of layered materials (Güemes et al. 2018). These same fiber-optic installations could be reused with DAS interrogators to measure the dynamic strain field related to high-frequency vibrations. Given additional insights yielded by dense accelerometer arrays in some applications, DAS may provide complementary information or added measurement precision.

6. EMERGING APPLICATIONS

DAS has had some use in several new applications over the past few years: cryosphere, marine geophysics, geodesy, tectonics, and geomechanics. These areas are garnering increased interest, and several new experiments are ongoing.

6.1. Cryosphere

Scientists have carried out a handful of DAS experiments studying cryosphere processes on lake ice, in permafrost, and on glaciers. An early test of surface DAS arrays that used a fiber-optic cable frozen into lake ice to verify the response of DAS to active sources followed expected distance and azimuth trends (Castongia et al. 2017). The coupling between the cable jackets and ice was strong enough that data quality using tight buffered cable was much better than loose-tube cable (i.e., coupling of fiber to jacket was a limiting factor). However, coupling between the cable and ground varies among cryosphere applications. Passive and active permafrost imaging were performed alongside a road in Alaska using data acquired by a trenched DAS array before and throughout a controlled thaw experiment (Martin et al. 2016, Ajo-Franklin et al. 2017, Wagner et al. 2018). These studies aimed to image the active layer at the scale of meters, motivated by the hazard posed to Arctic infrastructure by incipient talik formation. Experimenters noted challenges: spatially variable ground-to-cable coupling and the strong response of surface wave velocities to precipitation (Dou et al. 2016). However, along favorably oriented ray paths crossing the thaw zone, ambient noise analysis revealed that a refracted SV wave was less sensitive to precipitation and slowed by 50% to 350% throughout the thawing (Lindsey 2019). This experiment suggests DAS and ambient noise analysis could be used in future large-scale permafrost studies.

DAS has shown value on glaciated terrain, as was tested with a 1-km array on Rhonegletscher (Walter et al. 2020). This experiment demonstrated that coupling between the cable and ground was damped by snow depending on dry or wet snow conditions, and researchers hypothesize that this reduced sensitivity to high-frequency active source reflections. Despite this limitation, the density of the array enabled location and source estimation of a stick-slip event between the base of the ice and the bedrock, detection of a rockfall event, ambient noise analysis, and detection

of a surface crevasse icequake (Walter et al. 2020). Some cryosphere studies with DAS focused on surface arrays with large lateral extent, but borehole DAS arrays on glaciers provide access to depths of hundreds of meters to kilometers of ice thickness. For example, pressurized hot water drilling was used to deploy fiber to depths of more than 1 km at Store Glacier on Greenland Ice Sheet. This enabled detailed analysis of P- and S-wave velocities, Poisson's ratio, and anisotropy correlated to geological changes (Booth et al. 2020).

6.2. Marine Geophysics

Deepwater hydrocarbon reservoir imaging studies have used DAS through the underwater well-head for several years (Mateeva et al. 2013b, Shan et al. 2015, Lopez et al. 2017), sometimes with engineered cables and optical circulators to permit interrogator recording from shore (Muanenda 2018). More recently DAS has been used with seafloor cables to study the shallow ocean environment and subsurface, motivated in part by monitoring applications for geohazards, offshore hydrocarbon reservoirs, wind farms, and the security of telecommunications infrastructure.

In three contemporaneous studies, Williams et al. (2019), Sladen et al. (2019), and Lindsey et al. (2019) used onshore DAS IUs connected to subsea cables to sample earthquake wavefields, ocean microseisms, and ocean currents. The separate teams, each using a different scientific or wind farm fiber-optic cable and a different DAS interrogator, recovered between 4,192 and 9,986 points of seafloor ground motion spanning 20–42 km of horizontal cable range. One potential concern for seafloor earthquake recordings is strong ocean noise. Laboratory tests suggest that fiber-optic strain measurements may record less than 5% of true cable strain due to subsea fiber cable design features for robustness (Masoudi et al. 2019). However, teleseisms and regional earthquakes were recorded in all three subsea studies. The characteristically slower ocean wave phase speeds of 10 to 20 m/s enable f-k domain separation (Lindsey et al. 2019, Williams et al. 2019). According to Lindsey et al. (2019), body waves radiating from an M3.4 earthquake 40 km away were found to produce secondary seismic waves at mapped and unmapped fault locations, potentially due to conversion into Scholte waves or a fault zone trapping mechanism (Li & Leary 1990), and S waves slowed while passing through one fault zone.

The passive ocean seismic background was also evaluated in each submarine DAS experiment. From shore to 100 m depth, DAS observations around 0.05–0.25 Hz were consistent with dispersive landward-directed wind-wave loading described by gravity wave theory in shallow water, but in 2,500-km water depth, DAS amplitudes were 100-fold lower. Williams et al. (2019) showed that DAS sensor density permits analysis of small perturbations in surface gravity waves caused by ocean currents. At frequencies of 0.5 to 2 Hz and wavenumbers around $1\text{e-}3\text{ m}^{-1}$, linear symmetric components with Scholte wave velocity suggested in situ generation of secondary microseisms.

6.3. Geodesy, Tectonics, and Geomechanics

While many applications using DAS primarily focus on high-frequency dynamic strain measurements for imaging or seismic source analysis, DAS has also been applied to study low-frequency seismology and strain onshore and in marine environments. In hydraulic fracturing processes used at unconventional sites, fluid-sand mixtures are pumped into the subsurface to create or dilate existing fractures, which subsequently contract over minutes to hours. The strain field produced around a hydraulic fracturing stage thus has a timescale that is slower than conventional seismology but that is still time varying and so can be monitored with DAS. The total residual strain field will be the superposition of the large geomechanical changes in overburden stress as well as some very localized strain responses right at the fracture tip. Because strain is a spatial derivative of displacement, DAS can highlight small spatial-scale changes more than inertial or

surface geodetic displacement measurements (just as a velocity measurement highlights small temporal-scale changes more than displacement). This has been observed in computational geomechanics models (Sherman et al. 2019) as well as in the field with DAS installed behind casing or flute liners (Becker et al. 2017, Jin & Roy 2017).

Lower-frequency seismic signals can also be critical in monitoring slower natural hazard processes such as landslides. Broadband fiber-optic strain sensing is also making inroads into near-surface geomechanical monitoring applications, particularly detecting the potential for landslides before they produce irreversible damage (Iten 2012, Schenato et al. 2017). Moving forward, monitoring geomechanical and geodetic responses of rifts or faults along with any high-frequency signals using a single sensing system could give us an unprecedented view to map complex fracture networks and failure mechanisms, as well as volcanic deformation processes.

7. FUTURE COMMUNITY-SCALE NEEDS

DAS technology is currently permitting application of array methods to geophysical processes in new locations, but most geoscientists cannot use these data because (a) DAS data are shared only internally in groups that have instruments, (b) public seismology archives cannot support DAS data volumes, and (c) most geophysicists do not have the training or computational skillset to acquire, manage, or analyze DAS data effectively. Because of these three issues, we have an unequitable research environment, many data remain unexplored, and important geoscience discoveries are not happening. As outlined in **Figure 10**, the geoscience community must invest resources and efforts in ensuring that instrumentation is available and well characterized, that data can be widely and efficiently shared, that we take this opportunity to attract and retain diverse scientists, and that

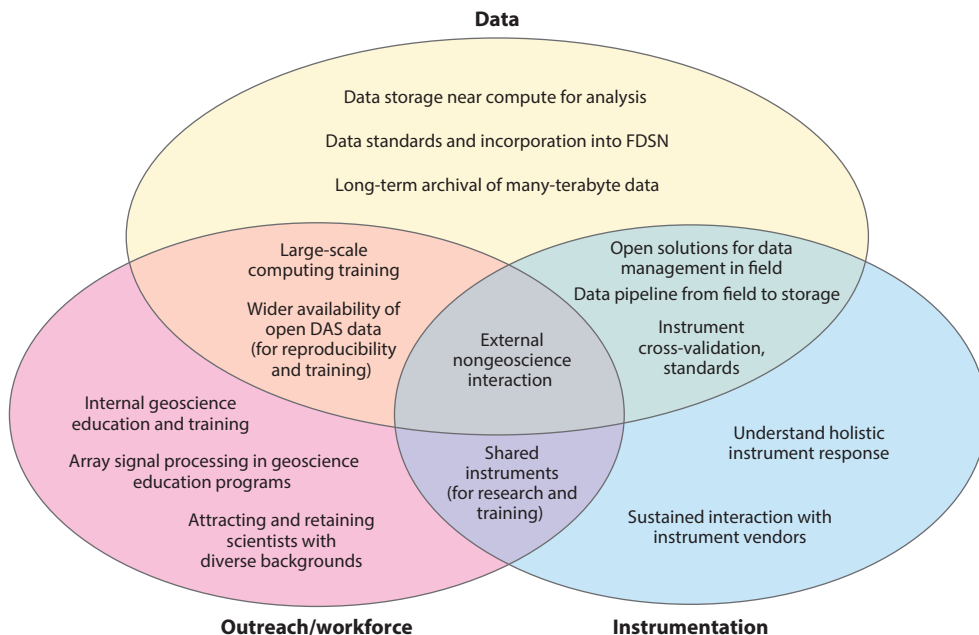


Figure 10

Venn diagram summary of data, workforce, and instrumentation needs in the DAS community. Abbreviations: DAS, distributed acoustic sensing; FDSN, International Federation of Digital Seismograph Networks.

training is available to prepare the broad community to acquire, analyze, and interpret large-scale DAS data.

DAS data are often stored in a hierarchical data format (e.g., HDF5 or PRODML) for efficient temporal or spatial data slicing, but a data standard has not been established. DAS data do not perfectly translate into existing multicomponent seismic data formats that store metadata per component (i.e., trace header) or per experiment (i.e., stream header). Additional fields are required to store information about the interrogator, the fiber and cable specifications, the total fiber length, gauge length, pulse repetition rate, laser wavelength, spatial and temporal averaging, and notes about the instrument's environment (e.g., vibration isolation table present or not). For complete data provenance, a future data standard should also track the tap-test events, DAS recording during tap-tests, and the choice of the tap locations to reproduce the channel mapping from the raw data.

Currently, most of the seismology community pulls data from shared public archives to local computing resources to process data on those local resources. As demonstrated in **Figure 2**, DAS data rates are several orders of magnitude higher than rates from nodal arrays. Were the IRIS Data Management Center (widely used by seismologists in the United States) to publicly host data from the Fiber-Optic foR Environment SENSing (FORESEE) array at Pennsylvania State University, this one experiment would require a roughly 10% increase in the capacity (Hutko et al. 2017, Zhu et al. 2020). Often DAS researchers store data on hard drives attached to the IU in the field. After fieldwork, disks are physically attached to local workstations for processing and analysis. A more efficient method used by some researchers is to load all data onto a High-Performance Computing (HPC) cluster. This amount of data (tens to hundreds of terabytes per experiment) would not be unusual for a large supercomputing center, but roadblocks arise on public data archives because they aim for data to be downloaded on demand from remote locations. Moving forward, having the ability to store large amounts of data alongside HPC resources (cluster or cloud) will be critical to enabling the seismology community to pursue scientific discovery with DAS.

DAS instrumentation access is currently limited. A few research groups negotiate directly with DAS instrument manufacturers (vendors) to either purchase or rent interrogators and accessory field equipment. In the larger seismology and geodesy community, geophysical instruments are freely available to academic researchers through shared community instrument pools. In the future, incorporating DAS instruments into a shared pool will be important to enable wider adoption and growth of the methodology. Two central motivations for DAS experiments are rapid deployments and long-term time-lapse capabilities, which will require coordinated shared instrument scheduling and prioritization.

Historically, seismologists have played an integral role in the design, testing, evaluation, and continued calibration of seismometers. To date, there has been a paucity of DAS cross-validation comparisons wherein multiple interrogators would be connected to different fibers within the same cable to understand performance trade-offs between optical setups and hardware components. Published quantitative results and data from this type of testing would inform the community about best practices in different applications.

Fibers can easily be deployed in populated areas and around infrastructure, so DAS provides unique opportunities for geophysics to grow into a more diverse and inclusive discipline. DAS can enable more geophysicists with limited mobility to carry out seismic acquisitions, both by bringing acquisition closer to infrastructure that supports access and by reducing physical labor requirements of large seismic instrument arrays. This could improve the inclusivity of geophysical fieldwork (Gilley et al. 2015). In addition to physical barriers to fieldwork, many geophysicists have been turned off of fieldwork due to negative past experiences in remote locations. Training for geophysicists with negative past experiences may provide an opportunity for a completely

different field experience in populated areas. Further, DAS should be used for geophysics outreach to students, future scientists, and residents of urban areas. In the United States, this outreach should particularly support neighborhoods and schools with large black, indigenous, or Latinx populations, as geophysics has thus far failed to attract and retain more researchers from these backgrounds (McDaris et al. 2018).

Successful DAS array deployment requires training that covers sensitivity to different wave modes, installation techniques in a variety of surface and subsurface deployments, and hands-on components related to optical parameters. Array seismology techniques must be more widely taught in universities; traditional techniques for analyzing individual or sparse sets of seismometers will miss geophysical information and often perform extremely inefficiently with the thousands of sensors available in a DAS experiment. This sentiment aligns with larger aims for more computational science training in geoscience programs to ensure that the time from data acquisition to geophysical insight is reasonable (Natl. Acad. Sci. Med. 2020).

FUTURE ISSUES

1. Community-shared instruments with education on instrumentation, array seismology, and computational methods will ensure growth of fiber-optic seismology.
2. Distributed acoustic sensing (DAS) data sets are often tens to hundreds of times larger than node-based experiments, challenging current models of data access, archiving, and analysis.
3. DAS measurement calibration is widely unavailable, and unreliable amplitude information is an issue for subsurface imaging, attenuation studies, and source inversion.
4. The geoscience community must capitalize on DAS to attract and retain diverse scientists with a wider range of experiences, abilities, and interests.

DISCLOSURE STATEMENT

E.R.M. has received research funding from the US Department of Energy for projects carried out in collaboration with Sentek Instrument and Luna Innovations. From 2016 to 2018 E.R.M.'s PhD studies were supported by industrial affiliates of the Stanford Exploration Project consortium and a Schlumberger Innovation Fellowship. Both N.J.L. and E.R.M. have carried out experiments and analyzed DAS data from both Silixa and OptaSense instruments provided at a discounted rate or as in-kind donations.

ACKNOWLEDGMENTS

N.J.L. was supported by the George Thompson Postdoctoral Fellowship, the National Science Foundation, Lawrence Berkeley National Laboratory through a lab-directed research development grant, and the US Department of Defense Strategic Environmental Research and Development Program. E.R.M. was funded in part by the US Department of Energy under grant DE-FE0091786 and a Phase 1 STTR grant with Luna Innovations, grant DE-SC0019630; a Luther and Alice Hamlett Junior Faculty Fellowship; and subcontract 4000175547 with UT-Battelle, LLC operating Oak Ridge National Laboratory. N.J.L. and E.R.M. would like to thank several of their collaborators for enlightening discussions on DAS technology during the writing of this

review, including Aleksei Titov, Horst Rademacher, Verónica Rodríguez Tribaldos, Ariel Lellouch, Ge Jin, Thomas Coleman, and Jonathan Ajo-Franklin. They would also like to acknowledge numerous colleagues for helpful discussions on these topics, particularly their colleagues involved in the DAS Research Coordination Network. N.J.L. and E.R.M. thank their collaborators on a recent letter outlining future community-scale DAS needs: Julia Correa, Patrick Paitz, Aleksei Titov, Danica Roth, and Ethan Williams.

LITERATURE CITED

- Ajo-Franklin JB, Dou S, Lindsey NJ, Daley T, Freifeld B, et al. 2017. Timelapse surface wave monitoring of permafrost thaw using distributed acoustic sensing and a permanent automated seismic source. *SEG Tech. Prog. Expand. Abstr.* 2017:5223–27
- Ajo-Franklin JB, Dou S, Lindsey NJ, Monga I, Tracy C, et al. 2019. Distributed acoustic sensing using dark fiber for near-surface characterization and broadband seismic event detection. *Sci. Rep.* 9:1328
- Baird A, Stork A, Horne S, Naldrett G, Kendall JM, et al. 2020. Characteristics of microseismic data recorded by distributed acoustic sensing (DAS) systems in anisotropic media. *Geophysics* 85:KS139–47
- Bakku S. 2015. *Fracture characterization from seismic measurements in a borehole*. PhD Thesis, Mass. Inst. Technol., Cambridge, MA
- Becker M, Ciervo C, Cole M, Coleman T, Mondanos M. 2017. Fracture hydromechanical response measured by fiber optic distributed acoustic sensing at milliHertz frequencies. *Geophys. Res. Lett.* 44:7295–302
- Becker MW, Ciervo C, Coleman T. 2018. Laboratory testing of low frequency strain measured by distributed acoustic sensing. *SEG Tech. Prog. Expand. Abstr.* 2018:4963–66
- Becker MW, Coleman TI. 2019. Distributed acoustic sensing of strain at Earth tide frequencies. *Sensors* 19:1975
- Benioff H. 1935. A linear strain seismograph. *Bull. Seismol. Soc. Am.* 25:283–309
- Berger J, Lovberg R. 1970. Earth strain measurements with a laser interferometer: An 800-meter Michelson interferometer monitors the earth's strain field on the surface of the ground. *Science* 170:296–303
- Biondi B, Martin E, Cole S, Karrenbach M, Lindsey N. 2017. Earthquakes analysis using data recorded by the Stanford DAS array. *SEG Tech. Prog. Expand. Abstr.* 2017:2752–56
- Blum JA, Noonan SL, Zumberge MA. 2008. Recording Earth strain with optical fibers. *IEEE Sens. J.* 8:1152–60
- Bona A, Dean T, Correa J, Pevzner R, Tertyshnikov K, Zaanen LV. 2017. Amplitude and phase response of DAS receivers. In *79th EAGE Conference and Exhibition in Paris, France*, pp. 1–5. Houten, Neth.: EAGE
- Booth A, Christoffersen P, Schoonman C, Clarke A, Hubbard B, et al. 2020. Distributed acoustic sensing (DAS) of seismic properties in a borehole drilled on a fast-flowing Greenlandic outlet glacier. *Geophys. Res. Lett.* 47:e2020GL088148
- Bucaro J, Dardy H, Carome E. 1977. Fiber-optic hydrophone. *J. Acoust. Soc. Am.* 62:1302–4
- Castongia E, Wang HF, Lord N, Fratta D, Mondanos M, Chalari A. 2017. An experimental investigation of distributed acoustic sensing (DAS) on lake ice. *J. Environ. Eng. Geophys.* 22:167–76
- Cedilnik G, Hunt R, Lees G. 2018. Advances in train and rail monitoring with DAS. *OSA Tech. Digest* 2018:ThE35
- Clements T, Denolle M. 2018. Tracking groundwater levels using the ambient seismic field. *Geophys. Res. Lett.* 45:6459–65
- Cole J, Johnson R, Bhuta P. 1977. Fiber-optic detection of sound. *J. Acoust. Soc. Am.* 62:1136–38
- Cole S, Karrenbach M, Kahn D, Rich J, Silver K, Langton D. 2018. Source parameter estimation from DAS microseismic data. *SEG Tech. Prog. Expand. Abstr.* 2018:4928–32
- Constantinou A, Farahani A, Cuny T, Hartog A. 2016. Improving DAS acquisition by real-time monitoring of wireline cable coupling. *SEG Tech. Prog. Expand. Abstr.* 2016:5603–7
- Correa J, Pevzner R, Bona A, Tertyshnikov K, Freifeld B, et al. 2019. 3D vertical seismic profile acquired with distributed acoustic sensing on tubing installation: a case study from the CO₂CRC Otway Project. *Interpretation* 7:SA11–19
- Dakin J. 1990. *Distributed fibre optic sensor system*. UK Patent, GB2222247A

- Daley T, Freifeld B, Ajo-Franklin J, Dou S, Pevzner R, et al. 2013. Field testing of fiber-optic distributed acoustic sensing (DAS) for subsurface seismic monitoring. *Leading Edge* 32:936–42
- Daley T, Miller D, Dodds K, Cook P, Freifeld B. 2016. Field testing of modular borehole monitoring with simultaneous distributed acoustic sensing and geophone vertical seismic profiles at Citronelle, Alabama. *Geophys. Prospect.* 64:1318–34
- Daley T, Solbau R, Ajo-Franklin J, Benson S. 2007. Continuous active-source seismic monitoring of CO₂ injection in a brine aquifer. *Geophysics* 72:A57–61
- Dean T, Cuny T, Hartog AH. 2017. The effect of gauge length on axially incident P-waves measured using fibre optic distributed vibration sensing. *Geophys. Prospect.* 65:184–93
- DeWolf S, Wyatt FK, Zumberge MA, Hatfield W. 2015. Improved vertical optical fiber borehole strainmeter design for measuring Earth strain. *Rev. Sci. Instrum.* 86:114502
- Dou S, Ajo-Franklin J, Daley T, Robertson M, Wood T, Freifeld B. 2016. Surface orbital vibrator (SOV) and fiber-optic DAS: field demonstration of economical, continuous-land seismic time-lapse monitoring from the Australian CO₂CRC Otway site. *SEG Tech. Prog. Expand. Abstr.* 2016:5552–56
- Dou S, Lindsey N, Wagner A, Daley T, Freifeld B, et al. 2017. Distributed acoustic sensing for seismic monitoring of the near surface: a traffic-noise interferometry example. *Sci. Rep.* 7:11620
- Egorov A, Pevzner R, Bóna A, Glubokobskikh S, Puzyrev V, et al. 2017. Time-lapse full waveform inversion of vertical seismic profile data: workflow and application to the CO₂CRC Otway project. *Geophys. Res. Lett.* 44:7211–18
- Eickhoff W, Ulrich R. 1981. Optical frequency domain reflectometry in single-mode fiber. *Appl. Phys. Lett.* 39:693–95
- Fang G, Li Y, Zhao Y, Martin E. 2020. Urban near-surface seismic monitoring using distributed acoustic sensing. *Geophys. Res. Lett.* 47:e2019GL086115
- Farhadiroushan M, Parker TR, Shatalin S. 2009. *Method and apparatus for optical sensing*. US Patent WO2010136810A2
- Fernández-Ruiz MR, Soto MA, Williams EF, Martin-Lopez S, Zhan Z, et al. 2020. Distributed acoustic sensing for seismic activity monitoring. *APL Photonics* 5:030901
- Frignet B, Hartog A, Mackie D, Kotov O, Liokumovich L. 2014. Distributed vibration sensing on optical fibre: field testing in borehole seismic applications. *Proc. SPIE* 9157:91575N
- Gabai H, Eyal A. 2016. On the sensitivity of distributed acoustic sensing. *Opt. Lett.* 41:5648–51
- Gilley B, Atchison C, Feig A, Stokes A. 2015. Impact of inclusive field trips. *Nat. Geosci.* 8:579–80
- Güemes A, Fernández-López A, Díaz-Maroto P, Lozano A, Sierra-Perez J. 2018. Structural health monitoring in composite structures by fiber-optic sensors. *Sensors* 18:1094
- Harris K, White D, Samson C. 2017. Imaging the Aquistore reservoir after 36 kilotonnes of CO₂ injection using distributed acoustic sensing. *Geophysics* 82:M81–96
- Hartog A. 2017. *An Introduction to Distributed Optical Fibre Sensors*. Boca Raton, FL: CRC
- Hartog A, Frignet B, Mackie D, Clark M. 2014. Vertical seismic optical profiling on wireline logging cable. *Geophys. Prospect.* 62:693–701
- Huot F, Biondi B, Beroza G. 2018a. Jump-starting neural network training for seismic problems. *SEG Tech. Prog. Expand. Abstr.* 2018:2191–95
- Huot F, Martin E, Biondi B. 2018b. Automated ambient noise processing applied to fiber optic seismic acquisition (DAS). *SEG Tech. Prog. Expand. Abstr.* 2018:4688–92
- Hutko A, Bahavar M, Trabant C, Weekly R, Van Fossen M, Ahern T. 2017. Data products at the IRIS-DMC: growth and usage. *Seismol. Res. Lett.* 88:892–903
- Inbal A, Cristea-Platon T, Ampuero JP, Hillers G, Agnew D, Hough SE. 2018. Sources of long-range anthropogenic noise in southern California and implications for tectonic tremor detection. *Bull. Seismol. Soc. Am.* 108:3511–27
- Iten M. 2012. *Novel Applications of Distributed Fiber-Optic Sensing in Geotechnical Engineering*. Zurich: vdf Hochschulverlag AG
- Jakkampudi S, Shen J, Li W, Dev A, Zhu T, Martin E. 2020. Footstep detection in urban seismic data with a convolutional neural network. *Leading Edge* 39:654–60
- Jin G, Roy B. 2017. Hydraulic-fracture geometry characterization using low-frequency DAS signal. *Leading Edge* 36:975–80

- Jousset P, Reinsch T, Ryberg T, Blanck H, Clarke A, et al. 2018. Dynamic strain determination using fibre-optic cables allows imaging of seismological and structural features. *Nat. Commun.* 9:2509
- Karrenbach M, Cole S, Ridge A, Boone K, Kahn D, et al. 2018. Fiber-optic distributed acoustic sensing of microseismicity, strain and temperature during hydraulic fracturing. *Geophysics* 84:D11–23
- Karrenbach M, Kahn D, Cole S, Ridge A, Boone K, et al. 2017. Hydraulic-fracturing-induced strain and microseismic using in situ distributed fiber-optic sensing. *Leading Edge* 36:837–44
- Kishida K, Yamauchi Y, Guzik A. 2014. Study of optical fibers strain-temperature sensitivities using hybrid Brillouin-Rayleigh system. *Photonic Sens.* 4:1–11
- Kiyashchenko D, Mateeva A, Duan Y, Johnson D, Pugh J, et al. 2020. Frequent 4D monitoring with DAS 3D VSP in deep water to reveal injected water-sweep dynamics. *Leading Edge* 39:471–79
- Kong Q, Allen RM, Schreier L, Kwon YW. 2016. Myshake: a smartphone seismic network for earthquake early warning and beyond. *Sci. Adv.* 2:e1501055
- Kowarik S, Hussels MT, Chruscicki S, Münzenberger S, Lämmerhirt A, et al. 2020. Fiber optic train monitoring with distributed acoustic sensing: conventional and neural network data analysis. *Sensors* 20:450
- Kreger ST, Klein JW, Rahim NAA, Bos JJ. 2015. Distributed Rayleigh scatter dynamic strain sensing above the scan rate with optical frequency domain reflectometry. *Proc. SPIE* 9480:948006
- Kuvshinov B. 2016. Interaction of helically wound fibre-optic cables with plane seismic waves. *Geophys. Prospect.* 64:671–88
- Lancelle C. 2016. *Distributed acoustic sensing for imaging near-surface geology and monitoring traffic at Garner Valley, California*. PhD Thesis, Univ. Wisconsin–Madison, Madison, WI
- Lellouch A, Lindsey NJ, Ellsworth WL, Biondi BL. 2020a. Comparison between distributed acoustic sensing and geophones: downhole microseismic monitoring of the FORGE geothermal experiment. *Seismol. Res. Lett.* 91(6):3256–68
- Lellouch A, Meadows MA, Nemeth T, Biondi B. 2020b. Fracture properties estimation using digital acoustic sensing recording of guided waves in unconventional reservoirs. *Geophysics* 85:M85–95
- Lellouch A, Yuan S, Spica Z, Biondi B, Ellsworth W. 2019. Seismic velocity estimation using passive downhole distributed acoustic sensing records: examples from the San Andreas Fault Observatory at Depth. *J. Geophys. Res. Solid Earth* 124:6931–48
- Li YG, Leary P. 1990. Fault zone trapped seismic waves. *Bull. Seismol. Soc. Am.* 80:1245–71
- Li Z, Zhan Z. 2018. Pushing the limit of earthquake detection with distributed acoustic sensing and template matching: a case study at the Brady geothermal field. *Geophys. J. Int.* 215:1583–93
- Lim Chen Ning I, Sava P. 2018. Multicomponent distributed acoustic sensing: concept and theory. *Geophysics* 83:P1–8
- Lin FC, Li D, Clayton RW, Hollis D. 2013. High-resolution 3D shallow crustal structure in Long Beach, California: application of ambient noise tomography on a dense seismic array. *Geophysics* 78:Q45–56
- Lindsey N. 2019. *Fiber-optic seismology in theory and practice*. PhD Thesis, Univ. Calif., Berkeley
- Lindsey NJ, Dawe TC, Ajo-Franklin JB. 2019. Illuminating seafloor faults and ocean dynamics with dark fiber distributed acoustic sensing. *Science* 366:1103–7
- Lindsey NJ, Martin ER, Dreger DS, Freifeld B, Cole S, et al. 2017. Fiber-optic network observations of earthquake wavefields. *Geophys. Res. Lett.* 44:11792–99
- Lindsey NJ, Rademacher H, Ajo-Franklin JB. 2020. On the broadband instrument response of fiber-optic DAS arrays. *J. Geophys. Res. Solid Earth* 125:e2019JB018145
- Lopez J, Mateeva A, Chalenski D, Przybysz-Jarnut J. 2017. Valuation of distributed acoustic sensing VSP for frequent monitoring in deepwater. *SEG Tech. Prog. Expand. Abstr.* 2017:6044–48
- Luo B, Trainor-Guitton W, Bozdağ E, LaFlame L, Cole S, Karrenbach M. 2020. Horizontally orthogonal distributed acoustic sensing array for earthquake- and ambient-noise-based multichannel analysis of surface waves. *Geophys. J. Int.* 222:2147–62
- Marra G, Clivati C, Luckett R, Tampellini A, Kronjäger J, et al. 2018. Ultraprecise laser interferometry for earthquake detection with terrestrial and submarine cables. *Science* 361:486–90
- Martin E. 2018. *Passive imaging and characterization of the subsurface with distributed acoustic sensing*. PhD Thesis, Stanford Univ., Stanford, CA
- Martin E, Ajo-Franklin J, Lindsey N, Daley T, Freifeld B, et al. 2015. Applying interferometry to ambient seismic noise recorded by a trenced distributed acoustic sensing array. *SEP* 158:247–54

- Martin E, Castillo C, Cole S, Sawasdee P, Yuan S, et al. 2017a. Seismic monitoring leveraging existing telecom infrastructure at the SDASA: active, passive, and ambient-noise analysis. *Leading Edge* 36:1025–31
- Martin E, Castillo C, Cole S, Sawasdee P, Yuan S, et al. 2017b. Seismic monitoring leveraging existing telecom infrastructure at the Stanford distributed acoustic sensing array: active, passive and ambient noise analysis. *Leading Edge* 36:1025–31
- Martin E, Huot F, Ma Y, Cieplicki R, Cole S, et al. 2018a. A seismic shift in scalable acquisition demands new processing: fiber-optic seismic signal retrieval in urban areas with unsupervised learning for coherent noise removal. *IEEE Signal Proc. Mag.* 35:31–40
- Martin E, Lindsey N, Ajo-Franklin J, Biondi B. 2018b. Introduction to interferometry of fiber optic strain measurements. EarthArXiv. <https://doi.org/10.31223/osf.io/s2tjd>
- Martin E, Lindsey N, Dou S, Ajo-Franklin J, Wagner A, et al. 2016. Interferometry of a roadside DAS array in Fairbanks, AK. *SEG Tech. Prog. Expand. Abstr.* 2016:2725–29
- Martins HF, Fernández-Ruiz MR, Costa L, Williams E, Zhan Z, et al. 2019. *Monitoring of remote seismic events in metropolitan area fibers using distributed acoustic sensing (DAS) and spatiotemporal signal processing*. Paper presented at the Optical Fiber Communication Conference, Optical Society of America, San Diego, CA, Mar. 3
- Masoudi A, Belal M, Newson T. 2013. A distributed optical fibre dynamic strain sensor based on phase-OTDR. *Meas. Sci. Technol.* 24:085204
- Masoudi A, Newson TP. 2016. Contributed review: distributed optical fibre dynamic strain sensing. *Rev. Sci. Instrum.* 87:011501
- Masoudi A, Pilgrim JA, Newson TP, Brambilla G. 2019. Subsea cable condition monitoring with distributed optical fiber vibration sensor. *J. Lightwave Technol.* 37:1352–58
- Mateeva A, Lopez J, Chalenski D, Tatanova M, Zwartjes P, et al. 2017. 4D DAS VSP as a tool for frequent seismic monitoring in deep water. *Leading Edge* 36:995–1000
- Mateeva A, Lopez J, Mestayer J, Wills P, Cox B, et al. 2013a. Distributed acoustic sensing for reservoir monitoring with VSP. *Leading Edge* 32:1278–83
- Mateeva A, Lopez J, Potters H, Mestayer J, Cox B, et al. 2014. Distributed acoustic sensing for reservoir monitoring with vertical seismic profiling. *Geophys. Prospect.* 62:679–92
- Mateeva A, Mestayer J, Cox B, Kiyashchenko D, Wills P, et al. 2012. Advances in distributed acoustic sensing (DAS) for VSP. *SEG Tech. Prog. Expand. Abstr.* <https://doi.org/10.1190/segam2012-0739.1>
- Mateeva A, Mestayer J, Yang Z, Lopez J, Wills P, et al. 2013b. Dual-well 3D VSP in deepwater made possible by DAS. *SEG Tech. Prog. Expand. Abstr.* 2013:5062–66
- McDaris J, Manduca C, Iverson E, Huyck Orr C. 2018. Looking in the right places: minority-serving institutions as sources of diverse Earth science learners. *J. Geosci. Educ.* 65:407–15
- Mestayer J, Cox B, Wills P, Kiyashchenko D, Lopez J, et al. 2011. Field trials of distributed acoustic sensing for geophysical monitoring. *SEG Tech. Prog. Expand. Abstr.* 2011:4253–57
- Milne D, Masoudi A, Ferro E, Watson G, Le Pen L. 2020. An analysis of railway track behaviour based on distributed optical fibre acoustic sensing. *Mech. Syst. Sign. Proc.* 142:106769
- Minardo A, Porcaro G, Giannetta D, Bernini R, Zeni L. 2013. Railway traffic monitoring using Brillouin distributed sensors. *Proc. SPIE* 8794:87943C
- Muanenda Y. 2018. Recent advances in distributed acoustic sensing based on phase-sensitive optical time domain reflectometry. *J. Sens.* 2018:3897873
- Munn JD, Coleman TI, Parker BL, Mondanos MJ, Chalari A. 2017. Novel cable coupling technique for improved shallow distributed acoustic sensor VSPs. *J. Appl. Geophys.* 138:72–79
- Natl. Acad. Sci. Med. 2020. *A Vision for NSF Earth Sciences 2020–2030: Earth in Time*. Washington, DC: Natl. Acad.
- Paitz P, Sager K, Fichtner A. 2018. Rotation and strain ambient noise interferometry. *Geophys. J. Int.* 216:1938–52
- Papp B, Donno D, Martin JE, Hartog AH. 2017. A study of the geophysical response of distributed fibre optic acoustic sensors through laboratory-scale experiments. *Geophys. Prospect.* 65:1186–204
- Parker T, Shatalin S, Farhadiroushan M. 2014. Distributed acoustic sensing—a new tool for seismic applications. *First Break* 32:61–69

- Pelecanos L, Soga K, Elshafie M, de Battista N, Kechavari C, et al. 2018. Distributed fiber optic sensing of axially loaded bored piles. *J. Geotech. Geoenviron. Eng.* 144:04017122
- Peng F, Duan N, Rao YJ, Li J. 2014. Real-time position and speed monitoring of trains using phase-sensitive OTDR. *IEEE Photonics Technol. Lett.* 26:2055–57
- Posey R, Johnson G, Vohra S. 2000. Strain sensing based on coherent Rayleigh scattering in an optical fibre. *Electron. Lett.* 36:1688–89
- Rodríguez Tribaldos V, Ajo-Franklin J, Dou S, Lindsey N, Ulrich C, et al. 2020. Surface wave imaging using distributed acoustic sensing deployed on dark fiber: moving beyond high frequency noise. *EarthArXiv*. <https://doi.org/10.31223/osf.io/jb2na>
- Rost S, Thomas C. 2002. Array seismology: methods and applications. *Rev. Geophys.* 40:2–1–2–27
- Schenato L, Palmieri L, Camporese M, Bersan S, Cola S, et al. 2017. Distributed optical fibre sensing for early detection of shallow landslides triggering. *Sci. Rep.* 7:14686
- Schmandt B, Clayton RW. 2013. Analysis of teleseismic P waves with a 5200-station array in Long Beach, California: evidence for an abrupt boundary to inner borderland rifting. *J. Geophys. Res. Solid Earth* 118:5320–38
- Shan G, Kommedal J, Nahm J. 2015. VSP field trials of distributed acoustic sensing in Trinidad and Gulf of Mexico. *SEG Tech. Prog. Expand. Abstr.* 2015:5539–43
- Shapiro N, Campillo M. 2004. Emergence of broadband Rayleigh waves from correlations of the ambient seismic noise. *Geophys. Res. Lett.* 31:L07614
- Sherman C, Mellors R, Morris J, Ryerson F. 2019. Geomechanical modeling of distributed fiber-optic sensor measurements. *Interpretation* 7:SA21–27
- Sladen A, Rivet D, Ampuero JP, De Barros L, Hello Y, et al. 2019. Distributed sensing of earthquakes and ocean-solid Earth interactions on seafloor telecom cables. *Nat. Commun.* 10:5777
- Soga K, Luo L. 2018. Distributed fiber optics sensors for civil engineering infrastructure sensing. *J. Struct. Integr. Maint.* 3:1–21
- Spica Z, Pertom M, Martin E, Beroza G, Biondi B. 2020. Urban seismic site characterization by fiber-optic seismology. *J. Geophys. Res. Solid Earth* 125:e2019JB018656
- Spikes KT, Tisato N, Hess TE, Holt JW. 2019. Comparison of geophone and surface-deployed distributed acoustic sensing seismic data. *Geophysics* 84:A25–29
- Timofeev AV. 2015. Monitoring the railways by means of C-OTDR technology. *Int. J. Mech. Aerosp. Ind. Mechatron. Eng.* 9:634–37
- Wagner AM, Lindsey NJ, Dou S, Gelvin A, Saari S, et al. 2018. Permafrost degradation and subsidence observations during a controlled warming experiment. *Sci. Rep.* 8:10908
- Walter F, Gräff D, Lindner F, Paitz P, Köpfl M, et al. 2020. Distributed acoustic sensing of microseismic sources and wave propagation in glaciated terrain. *Nat. Commun.* 11:2436
- Wang H, Zeng X, Miller D, Fratta D, Feigle K, et al. 2018. Ground motion response to a M_L 4.3 earthquake using co-located distributed acoustic sensing and seismometer arrays. *Geophys. J. Int.* 312:2020–36
- Wang X, Williams E, Karrenbach M, González Herráez M, Fidalgo Martins H, Zhan Z. 2020. Rose parade seismology: signatures of floats and bands on optical fiber. *Seismol. Res. Lett.* 91:2395–98
- Webster P, Wall J, Perkins C, Molenaar M. 2013. Micro-seismic detection using distributed acoustic sensing. *SEG Tech. Prog. Expand. Abstr.* 2013:2459–63
- Wheeler LN, Take WA, Hoult NA, Le H. 2019. Use of fiber optic sensing to measure distributed rail strains and determine rail seat forces under a moving train. *Can. Geotech. J.* 56:1–13
- Wiesmeyr C, Litzemberger M, Waser M, Papp A, Garn H, et al. 2020. Real-time train tracking from distributed acoustic sensing data. *Appl. Sci.* 10:448
- Williams EF, Fernández-Ruiz MR, Magalhaes R, Vanthillo R, Zhan Z, et al. 2019. Distributed sensing of microseisms and teleseisms with submarine dark fibers. *Nat. Commun.* 10:5778
- Woolard A, Tarazaga P. 2018. Applications of dispersion compensation for indoor vibration event localization. *J. Vib. Control* 24:5108–17
- Yavuz S, Freifeld B, Pevzner R, Dzunic A, Ziramov S, et al. 2019. The initial appraisal of buried DAS system in CO2CRC Otway Project: the comparison of buried standard fibre-optic and helically wound cables using 2D imaging. *Explor. Geophys.* 50:12–21

- Yu C, Zhan Z, Lindsey NJ, Ajo-Franklin JB, Robertson M. 2019. The potential of DAS in teleseismic studies: insights from the Goldstone experiment. *Geophys. Res. Lett.* 46:1320–28
- Yuan S, Lellouch A, Clapp R, Biondi B. 2020. Near-surface characterization using a roadside distributed acoustic sensing array. arXiv:2006.01360 [physics.geo-ph]
- Zeng X, Lancelle C, Thurber C, Fratta D, Wang H, et al. 2017. Properties of noise cross-correlation functions obtained from a distributed acoustic sensing array at Garner Valley, California. *Bull. Seismol. Soc. Am.* 107:603–10
- Zeng X, Thurber C, Wang H, Fratta D, Matzel E, PoroTomo Team. 2016. *High-resolution shallow structure revealed with ambient noise tomography on a dense array*. Paper presented at the 42nd Workshop on Geothermal Reservoir Engineering, Stanford, CA, Feb. 13–15
- Zhang CC, Shi B, Gu K, Liu SP, Wu JH, et al. 2018. Vertically distributed sensing of deformation using fiber optic sensing. *Geophys. Res. Lett.* 45:11732–41
- Zhirnov A, Fedorov A, Stepanov K, Nesterov E, Karasik V, et al. 2016. Effects of laser frequency drift in phase-sensitive optical time-domain reflectometry fiber sensors. arXiv:1604.08854 [physics.ins-det]
- Zhou J, Pan Z, Ye Q, Cai H, Qu R, Fang Z. 2013. Characteristics and explanations of interference fading of a ϕ -OTDR with a multi-frequency source. *J. Lightwave Technol.* 31:2947–54
- Zhu T, Shen J, Martin ER. 2020. Sensing Earth and environment dynamics by telecommunication fiber-optic sensors: an urban experiment in Pennsylvania USA. *Solid Earth Discuss.* <https://doi.org/10.5194/se-2020-103>
- Zhu T, Stensrud DJ. 2019. Characterizing thunder-induced ground motions using fiber-optic distributed acoustic sensing array. *J. Geophys. Res. Atmos.* 124:12810–23
- Zumberge MA, Hatfield W, Wyatt FK. 2018. Measuring seafloor strain with an optical fiber interferometer. *Earth Space Sci.* 5:371–79
- Zumberge MA, Wyatt FK, Dong XY, Hanada H. 1988. Optical fibers for measurement of Earth strain. *Appl. Opt.* 27:4131–38

Contents

Minoru Ozima: Autobiographical Notes <i>Minoru Ozima</i>	1
The Geodynamic Evolution of Iran <i>Robert J. Stern, Hadi Shafaii Moghadam, Mortaza Pirouz, and Walter Mooney</i>	9
Subduction-Driven Volatile Recycling: A Global Mass Balance <i>D.V. Bekaert, S.J. Turner, M.W. Broadley, J.D. Barnes, S.A. Halldórsson, J. Labidi, J. Wade, K.J. Walowski, and P.H. Barry</i>	37
Atmospheric Loss to Space and the History of Water on Mars <i>Bruce M. Jakosky</i>	71
Climate Risk Management <i>Klaus Keller, Casey Helgeson, and Vivek Srikrishnan</i>	95
Continental Drift with Deep Cratonic Roots <i>Masaki Yoshida and Kazunori Yoshizawa</i>	117
Contemporary Liquid Water on Mars? <i>James J. Wray</i>	141
Geologically Diverse Pluto and Charon: Implications for the Dwarf Planets of the Kuiper Belt <i>Jeffrey M. Moore and William B. McKinnon</i>	173
The Laurentian Great Lakes: A Biogeochemical Test Bed <i>Robert W. Sterner</i>	201
Clocks in Magmatic Rocks <i>Fidel Costa</i>	231
Hydration and Dehydration in Earth's Interior <i>Eiji Ohtani</i>	253
Past Warmth and Its Impacts During the Holocene Thermal Maximum in Greenland <i>Yarrow Axford, Anne de Vernal, and Erich C. Osterberg</i>	279
Fiber-Optic Seismology <i>Nathaniel J. Lindsey and Eileen R. Martin</i>	309
Earth's First Redox Revolution <i>Chadlin M. Ostrander, Aleisha C. Johnson, and Ariel D. Anbar</i>	337

Toward an Integrative Geological and Geophysical View of Cascadia Subduction Zone Earthquakes <i>Maureen A.L. Walton, Lydia M. Staisch, Tina Dura, Jessie K. Pearl, Brian Sherrod, Joan Gomberg, Simon Engelhart, Anne Trébu, Janet Watt, Jon Perkins, Robert C. Witter, Noel Bartlow, Chris Goldfinger, Harvey Kelsey, Ann E. Morey, Valerie J. Sabakian, Harold Tobin, Kelin Wang, Ray Wells, and Erin Wirth</i>	367
Recent Advances in Geochemical Paleo-Oxybarometers <i>Brian Kendall</i>	399
The Organic Isotopologue Frontier <i>Alexis Gilbert</i>	435
Olivine-Hosted Melt Inclusions: A Microscopic Perspective on a Complex Magmatic World <i>Paul J. Wallace, Terry Plank, Robert J. Bodnar, Glenn A. Gaetani, and Thomas Shea</i>	465
Architectural and Tectonic Control on the Segmentation of the Central American Volcanic Arc <i>Esteban Gazel, Kennet E. Flores, and Michael J. Carr</i>	495
Reactive Nitrogen Cycling in the Atmosphere and Ocean <i>Katy E. Altieri, Sarah E. Fawcett, and Meredith G. Hastings</i>	523
Submarine Landslides and Their Tsunami Hazard <i>David R. Tappin</i>	551
Titan's Interior Structure and Dynamics After the Cassini-Huygens Mission <i>Christophe Sotin, Klára Kalousová, and Gabriel Tobie</i>	579
Atmospheric CO ₂ over the Past 66 Million Years from Marine Archives <i>James W.B. Rae, Yi Ge Zhang, Xiaoqing Liu, Gavin L. Foster, Heather M. Stoll, and Ross D.M. Whiteford</i>	609
A 2020 Observational Perspective of Io <i>Imke de Pater, James T. Keane, Katherine de Kleer, and Ashley Gerard Davies</i>	643
An Atlas of Phanerozoic Paleogeographic Maps: The Seas Come In and the Seas Go Out <i>Christopher R. Scotese</i>	679

Errata

An online log of corrections to *Annual Review of Earth and Planetary Sciences* articles may be found at <http://www.annualreviews.org/errata/earth>